New materials of Khoratpithecus, a late Miocene hominoid from Nakhon Ratchasima Province, Northeastern Thailand, confirm its pongine affinities

Yaowalak Chaimanee, Vincent Lazzari, Chotima Yamee, Kantapon Suraprasit, Mana Rugbumrung, Kamol Chaivanich, Jean-Jacques Jaeger

New materials of *Khoratpithecus*, a late Miocene hominoid from Nakhon Ratchasima Province, Northeastern Thailand, confirm its pongine affinities

Yaowalak Chaimanee, Vincent Lazzari, Chotima Yamee, Kantapon Suraprasit, Mana Rugbumrung, Kamol Chaivanich, Jean-Jacques Jaeger

Keywords: Southeast Asia, Thailand, Miocene, orangutan, ape

This is the accepted version in Palaeontographica, Abteilung A: Palaeozoology – Stratigraphy

Article Vol. 323, Issues 4–6: 147–186, DOI: 10.1127/pala/2022/0129

Abstract

Khoratpithecus piriyai is a large-bodied hominoid documented from the late Miocene locality of Khorat sand pit in Nakhon Ratchasima province, northeastern Thailand that was previously known anatomically from a mandible fragment and a partial maxilla. Here we describe additional four mandible fragments and one hemi-maxilla, all of which originating from the same sedimentary unit. Most of these new specimens are assigned to *K. piriyai* based on their dentognathic morphology. However, one larger specimen forms the basis for the new species, *Khoratpithecus magnus* n. sp. These specimens provide important new information about *Khoratpithecus* and help to understand the morphological variability of this taxon, enabling us to propose an emended diagnosis for the genus. The absence of scars for the anterior digastric muscles, a uniquely derived character only shared with *Pongo*, characterizes all new lower jaws that preserved the base of the symphysis and constitutes a significant character for this genus, together with the strong robustness of the mandibular corpora. Some characters show high variation, such as the intercanine breadth of the lower jaws which, when reduced, induces a divergent shape of the tooth rows, a feature that also occurs in the closely related taxa, *Ankarapithecus* and *Sivapithecus.* This character is present in all new specimens referred to *K. piriyai.* The new species, *K. magnus,* displays many similarities with *Khoratpithecus piriyai*, but differs from it by its larger size, having a body mass estimated as 30% larger than that of *K. piriyai,* combined with several distinct dental characters, including higher crown height and length/width molar proportions. Its lower jaw displays canine alveolar sizes similar to those of the other individuals from the same locality, which are of smaller size. Therefore, these differences cannot be attributed to sexual dimorphism, justifying the erection of a new species. These specimens also shed new light on the feeding adaptation of this genus. Several characters, including the rather small P_3, reduced honing facets, thick enamel, large molar crowns, very robust mandibular corpora, high crowned

molars and a tendency for heavy wear on the cheek teeth, point to a dental adaptation for an abrasive diet similar to that of *Indopithecus*. However, the comparison between these two genera suggests that their similarities are the result of an adaptation to an abrasive diet, reflecting homoplasy within the pongid clade. The climatic and vegetational changes occurring in South Asia during the late Miocene probably instigated these adaptative changes among three different large-bodied hominoids, *Khoratpithecus*, *Indopithecus* and the unknown ancestor of *Gigantopithecus*.

Contents

1. Introduction

Khoratpithecus is a middle to late Miocene hominoid known from Thailand and Myanmar (CHAIMANEE et al. 2003, 2004, 2006, 2019 and JAEGER et al. 2011). It is considered to be more closely related to *Pongo* than to other fossil pongines, based on shared derived characters of its mandible, such as the absence of anterior digastric muscle scars, the symphyseal structure (CHAIMANEE et al. 2004) and the naso-alveolar clivus (CHAIMANEE et al. 2019). The oldest known *Khoratpithecus* species is *K. chiangmuanensis*, from the middle Miocene of Chiang Muan coal mine, northern Thailand (12.4–12.2 Ma; COSTER et al. 2010), which is documented only by a few isolated teeth (CHAIMANEE et al. 2003). Its dental anatomy displays striking resemblances with the extant orangutan based on its wrinkled enamel, large shovel-like I^1 and strong sexual dimorphism. The late Miocene (9–6 Ma) *K. piriyai* (TF 6223; CHAIMANEE et al. 2004) from Khorat sand pit in northeastern Thailand is represented by a nearly complete mandible lacking its incisors, left canine, and ascending rami. More recently, a maxilla of cf. *Khoratpithecus* (MFT-K176; CHAIMANEE et al. 2019) was discovered from the same area. It displays a unique nasoalveolar clivus morphology, most similar to those of *Pongo* and *Sivapithecus,* but its teeth are very worn. The late Miocene (10.4–8.8 Ma) hominoid from the Irrawaddy Formation in central Myanmar, *K. ayeyarwadyensis* (MFI-K171, JAEGER et al. 2011) is documented by a left hemi-mandible with P_3–M_2. It displays a more slender corpus and shorter symphysis with shorter planum alveolare and narrower incisor area than *K. piriyai*. In addition, an isolated right upper molar of *Khoratpithecus* sp. (MFI 89) was discovered from the same area. Recently, TAKAI et al. (2021) described a left mandible with worn $M_{2–3}$, M_1 fragment, root of P_4 and alveoli of C–P_3 (MZKB-K-001) from a nearby locality in Myanmar and referred it to Ponginae gen. et sp. indet.

Here we describe four new hominoid mandible fragments and one hemi-maxilla from the Khorat sand pits, Nakhon Ratchasima province, northeastern Thailand. These new specimens extend our knowledge of the genus *Khoratpithecus* and of its morphological variation. They enable a re-evaluation of the dental metrics and the jaws anatomy of this genus, and they also allow to test previous conclusions concerning its pongid attribution and its phylogenetic relationships with *Pongo*. The morphological variation observed on these new specimens also forms the basis for an emended diagnosis for this genus.

2. Material and methods

Geological setting

The fossils described here (Table 1) were recovered from sand pits along the Mun River in Nakhon Ratchasima Province (Khorat), northeastern Thailand. They are derived from the lower sand unit (CHAIMANEE et al. 2006), the same sedimentary unit that yielded the lower jaw of *K. piriyai* (holotype TF 6223; CHAIMANEE et al. 2004) and a maxilla (MFT-K176; CHAIMANEE et al. 2019). The sediments are organic-rich sands that have yielded abundant fossil tree trunks and wood fragments, associated with large mammal, turtle and crocodile remains. Fossil mammals discovered from these sand pits include *Hipparion*; the rhinocerotids *Alicornops complanatum*, *Acerorhinus paleosinensis*, *Acerorhinus porpani* and *Brachypotherium primense* (CHAIMANEE et al. 2004; DENG et al. 2013; HANDA et al. 2020); the proboscideans *Deinotherium, Prodeinotherium pentapotamiae, Gomphotherium* sp., cf. *Protanancus macinnesi*, *Sinomastodon* cf. *yangziensis, Sinomastodon* sp., *Stegolophodon*, primitive *Stegodon*, *Tetralophodon* sp. and *Zygolophodon* sp. (SAEGUSA et al. 2005; THASOD et al. 2012; DUANGKRAYOM et al. 2017); the pigs *Hippopotamodon* cf. *sivalensis* and *Propotamochoerus* cf. *hysudricus*; the anthracotheres *Merycopotamus medioximus*, *M. thachangensis* and *Microbunodon milaensis* (LIHOREAU et al. 2007; HANTA et al. 2008); the

giraffid *Bramatherium* sp. and the bovids *Selenoportax vexillarius, Selenoportax falconeri, Selenoportax* sp. and *Pachyportax giganteus* (NISHIOKA et al. 2014, 2020). According to this large mammal fauna, a late Miocene age can be proposed, between 9 and 6 Ma by correlations with the Dhok Pathan mammalian zone of the Siwaliks (northern India and Pakistan) (BARRY et al. 2002; CHAIMANEE et al. 2006). This fossiliferous sand unit corresponds to fluvial channel deposits of the paleo-Mun River system as indicated by the abundant crocodile and turtle remains. The paleoenvironment of this area must have corresponded to a swampy area mixed with closed woodland habitats according to the occurrence of the rhinocerotid *Brachypotherium*, which is considered a swamp dweller. The pollen assemblage, dominated by thermophilous trees and grassland, indicates a transitional environment between woodland to grassland (SEPULCHRE et al. 2010). However, pollen spectra are dominated by hydromorphic plants suggesting that large areas of the floodplain were covered by grasslands (CHAIMANEE et al. 2006).

Institutional abbreviations

MFT = Mission Franco-Thai, Collections of Chulalongkorn University, Thailand; TF = Thai fossil, the Department of Mineral Resources, Thailand; MFI = Mission French-Irrawaddy collection, MZKB-K = Zaykabar Museum, Yangon, Myanmar.

Measurements

Dental measurements have been taken using Mitutoyo digital calipers to the nearest 0.01 mm. Measurements of mesiodistal length (MD) correspond to the maximum values and buccolingual width (BL) were taken separately at the trigonid (trig) and talonid (tal) (Table 2). Bivariate plots of buccolingual breadth (BL) versus mesiodistal length (MD) of the molars were generated to compare molar size among species. Intercanine breadth is the measurement of the distance between the lingual sides of left and right lower canines at the alveolar level. The mandibular symphyseal sectional measurements were taken on a sagittal µCT cross-

section. The symphyseal length corresponds to the maximum distance between the most antero-superior point (infradentale) and the most inferior point of the symphysis (gnathion). The symphyseal breadth (thickness) of transverse tori was measured at the maximum breadth that was perpendicular to the symphyseal length at the superior and inferior transverse tori. The symphyseal inclination angle was measured as the inclination of the longest axis relative to the alveolar plane. These measurements and the mandibular dimensions are given in Table 3. Dental proportions (MD length/BL width x 100, in %)) of teeth compared with other hominoids are given in Table 4. The buccal maximum crown height (H) was measured at the metaconid in lower molar and at the paracone in upper molar, yielding relative crown height (RCH, H/BL x100, in %). The mandibular corpus height and breadth were measured at the position of each tooth. The mandibular robusticity index (RI, corpus breadth/corpus height x 100, in %) is presented in Table 5.

Photos

Images were taken with a Nikon D7200 camera with AF-S Micro Nikkor lens 60 mm-f/2, 8G ED, associated to a Stack-Short Cognysis equipment on rail, with a distance between each picture of 150 µm. Stacking has been made with the software *CombineZ.*

3D data acquisition and imaging

Specimens were scanned using an EasyTom HR-microtomograph (platform PLATINA of IC2MP, University of Poitiers, France) with 4320 projections, a frame rate of 12.5 fps, a frame averaging of 20, a voxel size of 49 µm, a voltage of 90 kV and a current of 260 µA. The resulting scan was reconstructed into TIFF stacks and was imported into Avizo 7 (FEI Visualization Sciences Group, Hillsboro, USA) for surface visualization and manipulation. The virtual volumes reconstructed from microtomographic images were then processed with VG Studiomax 1.2.1 (Volume Graphics, Heidelberg, Germany) software, in

order to generate virtual slices and to display internal characters, like symphysis, root and coronal section.

2D enamel thickness

A 2D segmentation of the enamel cap (EC) was possible for the virtual slices of M_2 of MFT-K177, MFT-K178, MFT-K181 and for M^2 of MFT-K180. The value for M^2 of MFT-K176 (CHAIMANEE et al. 2019) has been re-estimated. We computed virtual buccolingual cross-sections perpendicular to the tooth cervical plane and passing through the dentine horns of the protocone and paracone for the M^2, and entoconid and hypoconid for the M_2. The position of the dentine horn tips of the worn protocone and paracone were reconstructed by checking continuity of the marginal ridges beside these dentine horns. On these virtual cross-sections, we recorded the following measurements, using Fiji (SCHINDELIN et al. 2012) software: the length of the enamel-dentine junction (EDJ, in mm), the area of the enamel cap (EC, mm^2), and the area of the coronal dentine (CD, which includes the coronal pulp; in mm^2). From these measurements, we computed the 2D average enamel thickness index (AET, index in mm) which is the area of the enamel cap divided by the length of the EDJ, and the 2D relative enamel thickness index (RET, scale free index in %), which is the AET divided by the square root of the coronal dentine area (MARTIN 1985; OLEJNICZAK 2008).

Relative dentine horn height

The relative dentine horn height (RDHH) of the specimens was measured by the ratio of the height of the dentine horn on the total height of the dentine crown following OLEJNICZAK et al. (2008; Fig. 2). A mesial plane section was computed for each molar, as in our study of 2D enamel thickness. In these sections, the maximum height of the dentine was measured as a line perpendicular to the bi-cervical diameter and running to the dentine horn tip. The distance between the dentine horn tip and a line parallel to the bi-cervical diameter but running through the lowest point of the enamel-dentin junction in the occlusal basin was

also recorded. The heights of the paracone and the protocone were measured on the M^2, and the heights of the protoconid and the metaconid were measured on the M_2.

Body weight

We used the allometric equations of GINGERICH et al. (1982) based on tooth crown area (mesiodistal length, MD multiplied by buccolingual width, BL) of premolars and molars to estimate body mass. We also analyzed the summed area of the postcanine cheek teeth in relation to body weight for both the upper and lower dentition.

3. Systematic Paleontology

Order Primates LINNAEUS, 1758

Suborder Anthropoidea MIVART, 1864

Superfamily Hominoidea GRAY, 1825

Family Hominidae GRAY, 1825

Subfamily Ponginae ELLIOT, 1913

Genus *Khoratpithecus* CHAIMANEE et al., 2004

Type specimen: TF 6223, mandible fragment with well-preserved left P_3–M_3 and right C–M_3, the root alveoli of I_1 and root fragment of I_2 and left C.

Included species: *K. chiangmuanensis* CHAIMANEE et al. 2003; *K. piriyai* CHAIMANEE et al. 2004; *K. ayeyarwadyensis* JAEGER et al. 2011 and *K. magnus* n. sp. (this study).

Age and distribution: Middle to late Miocene age, Thailand and Myanmar.

Emended diagnosis: Large-bodied hominoid with estimated body mass between 24–74 kg. Nasoalveolar clivus long, nearly horizontally oriented with weak anteroposterior convexity and significant overlap with palatine process. Thin ‘knife edge’ clivus posterior pole associated with incisive fossa and canal larger than those of *Sivapithecus* and *Pongo*. Palate shallow and broad. Large incisive foramen partially partitioned with posterior border located

at the level of the distal canine crown. Posterior palate dorsally oriented with a distally located, large and oval greater palatine foramen. Upper incisors heteromorphic. Upper canines externally rotated. Premolars and molars with coarse enamel wrinkling. Premolar and molar cingula and cingulid absent. P^3 sub-rectangular in outline with reduced parastyle and parastyle area. Lingual and buccal walls of upper premolars and molars slanted with reduced anterior fovea. Upper molar crowns rather square or wider buccolingually than mesiodistally, with metacone more mesially located than hypocone and well-expressed crista obliqua. Mandible with high robusticity index, mandibular corpus bearing a strong lateral eminence at M_3 level, lacking scars for anterior digastric muscles and displaying highly variable intercanine breadth. Symphysis long and inclined (40°–48° in relation to the alveolar plane) extended to P_4 or M_1 level, with superior transverse torus thicker than inferior transverse torus, which is not elongated into a simian shelf. Lower premolars and molars with slanted buccal walls and reduced anterior foveae. P_3 posterior root oriented lingually.

Differential diagnosis: *Khoratpithecus* differs from other known hominoids, with the exception of *Pongo*, by its lack of anterior digastric muscle scars. Differs from *Ankarapithecus* and *Lufengpithecus* by having the posterior pole of the nasoalveolar clivus at the same level as the palate rather than being superior to the palate. Differs from *Ankarapithecus* by the transverse flatness of its nasal floor, shallower and dorsally inflected distal palate, more inclined symphysis with weaker superior transverse torus. Differs from *Lufengpithecu*s by its coarsely wrinkled enamel, more buccolingually extended M^1 and M^2 with reduced anterior foveae and narrow trigons, more rectangular P^3 occlusal shape, larger M_3, more inclined symphysis and stronger lateral eminence. Differs from *Sivapithecus* by its larger and partitioned incisive foramen, larger incisive canal and fossa, and more inclined symphysis with weaker superior transverse torus. Differs from *Indopithecu*s by its smaller size, more inclined symphysis, buccolingually wider lower molars and larger intercanine

breadth. Differs from *Gigantopithecu*s by its smaller size, more inclined symphysis, larger intercanine breadth and upper molar occlusal surface proportions. Differs from *Pongo* by its more robust jaws, shorter alveolar process of premaxilla, less convex clivus, larger incisive foramen canal and fossa, shallower anterior palate, shorter upper central incisor roots, smaller canines, more reduced intercanine breadth, more inclined and thicker symphysis with less elongated inferior transverse torus, less wrinkled enamel and stronger lateral eminence of its mandible.

Khoratpithecus piriyai Chaimanee et al., 2004

Type specimen: as in genus.

Locality and age: Khorat sand pit, Nakhon Ratchasima Province, northeastern Thailand, late Miocene, between 9 and 6 Ma.

Studied material: MFT-K177 (mandible), MFT-K181 (mandible) and MFT-K180 (maxilla).

Dimension: Tables 2–5.

Description:

Mandible MFT-K177

MFT-K177 is an almost entire lower jaw missing ascending rami, preserving complete left and right corpora and intact left P_4–M_3 and right P_3–M_3 (text-fig. 1). The incisors and canines are missing and the left P_3 is broken, only its roots being preserved. The left corpus has been broken vertically at the mesial part of M_1 (text-fig. 1D) and was fixed by glue but in an incorrect position. Therefore, we used a symmetric µCT image of the well-preserved right jaw to reconstitute the dental arcade. It appears that the virtual reconstruction of this mandible depicts the reality, indicating that the left jaw of this specimen is strongly deformed. The measurements of the distances between the tooth rows have been obtained from this µCT-reconstructed jaw. The dental arcade displays a narrow intercanine breadth (ca. 18.71 mm) and a maximum width at the most buccal points of M_3 (68.98 mm) (text-fig. 2).

Both corpora are well preserved, except the anterior part of the jaw, which is broken away, offering a view on the lingual walls of the alveoli of four incisor and two canine roots (text-fig. 1E). The corpora are very robust, with very prominent lateral eminences dominating at the levels of M_3. The corpus thickness and lateral prominence are massive on both sides and displays strong asymmetry, being more massive on the right side (Table 5). The roots of the ascending rami begin at the M_1/M_2 level. Both ascending rami are broken at a level slightly above the alveolar margin. The distal parts of M_3 are hidden by the ascending rami. The buccinator groove is wide, representing 120% (right) and 130% (left) of the M_3 breadth. In lateral view, the lateral part of mandibular corpus become significantly deeper posteriorly from P_3 to M_3, being shallowest at P_3 (ca. 31.80 mm) and deepest at M_3 (47.00 mm) (text-figs. 1D, 1F). Such an increase is rather peculiar and could not be observed in other Miocene hominoid fossils, which usually display similar deepness of the corpus from P_3 to M_3 or even greater deepness at the P_3 level than at M_3 (FUSS et al. 2017). Left and right mental foramina open under the apices of the mesial roots of P_3, about 16.1 mm below the alveolar margin and 6.40 mm above the corpus base. The distance between these mental foramina is about 29.36 mm (39.0 mm in TF 6223; Table 3). No post-canine-P_3 depression can be observed. In lingual view, the mylohyoid line is well marked and there is no smooth transition between the lingual part of the jaw and the medial pterygoid fossae, which are deep and separated from the anterior part of the corpus by a distinct sub-vertical ridge.

The coronal sections of MFT-K177 (text-fig. 3) are strong, distinct from all other known Asian hominoids (BROWN 1989). They display U-shape sections with vertical lateral flanges at the P_3/P_4 level, and a long and thick symphysis. The jaw develops a greater thickness and a bony swelling at M_1/M_2 level, below the proximal extremity of the oblique line. The coronal sections of the corpus display thick cortical bone, cancellous bone forming complex trabeculae, large central cavities, and highly distinctive outlines. MFT-K177 appears

to be extremely robust and displays very strong muscular insertions, which testify to a very massive masticatory complex suggesting a diet dominated by hard food. The very worn premolar and molar occlusal surfaces also confirms this interpretation.

The anterior part of the jaw is broken on its labial face (text-fig. 1E). However, the symphysis of MFT- K177 is significantly thick and the sublingual plane is relatively long, being extended until the distal level of M_1 (text-fig. 3C). Its sagittal section, observed from a virtual µCT image (text-fig. 4), is massive, slightly inclined (40° with the alveolar margin), with a thick superior transverse torus (25.0 mm), a well-marked genioglossal fossa and a thinner inferior transverse torus (17.5 mm; Table 3) which is not elongated into a simian shelf as in *Pongo*. The long planum alveolare slopes down about 30° until the genioglossal fossa. On the surface of the inferior transverse torus, which is well preserved, there are no traces of anterior digastric muscles insertion scars, the bone surface being completely smooth (text-fig. 1B).

Incisors and canines are missing but the lingual walls of their alveoli are sub-vertical (text-fig. 1E). The four incisor alveoli are similar in size and their root apices are about 1 cm shorter than the canine roots. The canines are large and their root apices nearly reach the base of the symphysis. The left canine alveolus is partly preserved on its lingual side and indicates that it was externally oriented.

The P_3-M_3 row is almost straight with a slight buccal concavity located at the M_1 level (text-fig. 1A). Premolar length represents about 33 % of the postcanine tooth length. The left P_3 crown is missing, with only parts of its roots being preserved. P_3 displays an oblique orientation of about 45° to the long axis. The right P_3 displays a tiny honing facet on its mesial wall. P_3 is worn but clearly displays a distinct metaconid cusp connected to the protoconid by a short transverse crest. Its mesial part is wider than its distal part. Its buccal wall is bent lingually. Its lingual wall is slightly convex due to the development of the

metaconid. A small parastylid is present and connected to a short mesiolingual cingulid that ends on the mesial flank of the metaconid, delimiting a small and shallow anterior fovea. A distal crest issued from the protoconid curves lingually, defining a narrow and tiny talonid basin which is filled by a few enamel wrinkles. It is separated from the distal wall of the metaconid by a tiny fissure. P_4 has a trapezoidal outline and is buccolingually wider at the trigonid level than at the talonid. The protoconid is the largest cusp and is situated opposite to the metaconid. On the left P_4, the protoconid is very worn, displaying a large and rounded dentine pit. The talonid is composed of two cusps, which are smaller and less elevated than the trigonid cusps. On both P_4, the buccal walls are slanted but the lingual walls are nearly vertical. A few enamel wrinkles can be observed in the reduced talonid basin.

The molars are mesiodistally elongated with a rectangular occlusal outline. The M_1 and M_2 do not differ in morphological details, but M_1 are more worn and smaller than M_2. Both are heavily worn, especially the right M_1, whose buccal side is deeply worn to the dentine level. The left M_1 has a deeply worn protoconid and a small rounded dentine pit on the hypoconid, which is located close to the protoconid and more anteriorly than the entoconid. Metaconid and entoconid are located on the apices of the vertical lingual wall, and molar wear surfaces appear to be more oblique from lingual to buccal, rather than horizontal. The buccal wall is slanted and less elevated. The lingual wall is vertical and smooth without any trace of cingulid. The hypoconulid is located on the buccal side and distal to the hypoconid. It is small and connected by two distinct arms to the entoconid, forming a small distal fovea. The M_2 is significantly larger than M_1. The mesial fovea is strongly reduced so that there is nearly no trace of it left at this stage of wear. The hypoconulid is more distal than on M_1 and a distinct posterior fovea exists. The hypoconid of left M_2 is very worn, displaying a large and rounded dentine pit, confirming a strongly asymmetric wear, also observed on the M_1. The M_3 crowns are rather elevated, like those of the M_1 and M_2. No dentine pit can be

observed on M_3. Its crown occlusal surface is larger than that of M_2. Their occlusal surfaces are also buccolingually oblique, but much less so than those of the anterior molars. The anterior fovea is closed, and the distal fovea is well developed. The hypoconulids are only slightly larger than those of M_2, so that there is no distally extended talonid basin. The M_3 crown is narrower than that of M_2. Its MD length/BL width ratio is 122 % (Table 4). The enamel thickness measured on M_2 falls into "thick category" based on Martin (1985), being thicker than on the *K. piriyai* holotype (TF 6223) (Table 6).

The µCT reconstructions show that the premolars have long roots (text-fig. 5). P_3 has two mesial and distal roots, both with bifid apices. The mesial root has a very thick mesiobuccal apex, slightly oriented mesially and its tip is bent lingually. The distal root is deeply divided but the distolingual apex is large and displaced lingually. P_4 has two long transversely oriented roots, which display bifid apices. P_4 roots are as long as those of the M_1. Each molar has two long mesial and distal roots, flattened, grooved and displaying bifid apices. M_3 roots are shorter and more massive than those of the anterior molars; the distal root of M_3 being the thickest and distally oriented.

Mandible MFT-K181

MFT-K181 is a left hemi-mandible including P_3 to M_3, the alveoli of I_1, I_2 and canine (text-fig. 6). The loss of alveolar bone on the buccal surfaces exposes the roots of the teeth from P_3 to M_2. The ascending ramus is broken behind the M_3.

The mandibular corpus is rather deep (45.93 mm under P_4; 49.31 mm under M_3) and thick, the mandibular robusticity index being 46% at P_4 level and 66 % at M_3 level (Table 5). The beginning of the masseteric fossa is preserved on a narrow area (1 cm wide), behind the lateral eminence and the oblique line. Its coronal section displays cancellous bone forming complex trabeculae surrounded by a thin layer of cortical bone. In addition, a cavity is developed inside the lower part of its corpus that extends from the M_2–M_3 level to the

symphysis. On its buccal side, two mental foramina are present, one under the canine root, and a larger one under the middle of P_3, 24.6 mm below the alveolar level (text-fig. 6C). A short postcanine-P_3 depression is developed under P_4 and M_1, but more posteriorly the corpus increases in thickness culminating at the lateral eminence. The strong oblique line arises from the lateral eminence and descends steeply toward the base of the corpus inferior to the level of another eminence located under M_2 trigonid where it continues horizontally until the P_4–M_1, and parallel to the base of the corpus. A wide (17.4 mm) buccinator groove is present and corresponds to 126% of M_3 maximal crown width.

The symphyseal section is exposed near its medial section due to the damage during fossilization (text-fig. 6D). It is thick (22.22 mm at the superior transverse torus and 16.8 mm at the inferior transverse torus) and long (>53.0 mm), it extends to the distal level of M_1 and is strongly inclined (45° with the alveolar margin) (Table 3) with a weakly marked genioglossal fossa. Its section is not elongated into a simian shelf as in *Pongo*. The long planum alveolare slopes down with an angle of 38° until the genioglossal fossa. On the lower surface of the well-preserved inferior transverse torus, there is no trace of anterior digastric muscle insertion scars, the bone surface being completely smooth (text-fig. 6B).

P_3–M_3 measures 67.18 mm, the premolars length (22.07 mm) representing 33 % of the tooth row. The teeth are slightly worn, without dentine pits. The canine alveolus is rather large, having a maximum transverse diameter of 19 mm and its long axis is oblique with respect to the postcanine tooth row. Its outline is subtriangular with rounded angles, being very slightly waisted in its middle part. The incisor roots are small, and their outlines and dimensions are similar to each other, measuring 12.43 mm in labiolingual and about 5.80 mm in mesiodistal diameter. The interalveolar septa separating canine from I_2 and I_2 from I_1 are thin and their root alveolar orientation is slightly procumbent. P_3 is large, with a high and lingually slanted protoconid connected to a small, low parastylid and a more distally located

small and low metaconid. On its mesial wall, there is a flat honing facet. Distally, a rather low but wide talonid basin is developed with a low hypoconid but no other cusp is individualized on the posterior shelf of the talonid basin. Its lingual wall displays fine enamel wrinkles as its talonid basin. P_4 buccal wall is also strongly slanted lingually. Its metaconid is as elevated as the protoconid and is separated from it by a small mesiodistal groove, but the protoconid is larger than the metaconid. A narrow anterior fovea is developed in front of these two cusps. The talonid, like that of P_3, displays fine enamel crenulations. It is lower than the trigonid and displays three small cusplets, corresponding to the hypoconid, the hypoconulid and the entoconid. The lingual wall of P_4 is nearly vertical, like those of the molars.

M_1 has a rectangular outline and its occlusal surface represents 70% of that of M_2. The metaconid is the highest cusp and is separated from the protoconid by a mesiodistal groove. A distinct anterior fovea is developed. The talonid has nearly the same elevation as the trigonid and shows a peripheralized entoconid. The hypoconid is the largest, among the distal cusps. The hypoconulid is located distally and develops a small lingual posterior fovea. M_2 is larger than M_1 and shows a similar occlusal surface morphology. M_3 has a similar size and shape as M_2 but a narrower talonid basin. Its MD length-BL width ratio is 127% (Table 4). Its trigonid buccal wall is strongly slanted lingually. No cingulids are developed on these molars. The enamel thickness measured on M_2 falls into "thick category" based on Martin (1985), being thicker than on the *K. piriyai* holotype (TF 6223) and slightly thicker than MFT-K177 (Table 6).

From µCT images, P_3 has two roots, a thick mesial root on the buccal side and a distal root which is long and strongly oriented lingually. P_4, M_1 and M_2 have two mesial and distal roots, which are flattened and grooved with bifid apices. M_2 has the longest roots. M_3 has two roots, the mesial root is flattened, grooved with bifid apices and the distal root is thick, massive and grooved (text-fig. 7).

Maxilla MFT-K180

MFT-K180 is a left maxilla of a young adult individual that preserves intact crowns of P^3–M^3 including parts of the alveolar bone, the facial surface and the root of the zygomatic process (text-fig. 8). The palatal process is missing, only one cm wide palatal bone shelf being preserved, showing the posterior palatine foramen located under the distal part of M^3. The anterior dentition area is missing, only the apex of I^2 root alveolus being preserved. The lower part of the canine jugum is preserved with a small part of the premaxilla. The inclination of the canine jugum is similar to that of MFT-K176 (CHAIMANEE et al. 2019) but its canine fossa, located above P^4 roots, is more deeply excavated. The maxilla between I^2 and C^1 has a smooth surface, but above the premolars and molars the surface becomes more rugose and irregular due to visible root contours and fenestrae. In superior view, the maxillary sinus is preserved in its anterior part and its floor displays no loculi or complete transverse septa and is not penetrated by the molar root tips (text-fig. 8B). The maxillary sinus is large, starting at the level of the mesial part of M^1 and enlarging posteriorly to the posterior preserved portion of the maxilla, distal to M^3. Its anterior margin is located about 15 mm posterior to the apex of the canine root. It extends into the zygomatic processes of the maxilla. The thickness of bone between the maxillary sinuses and the outer surface of the zygomatic roots is about 9.5 mm. The departure of the zygomatic branch of the maxilla is broken and located 17.2 mm above the M^2 alveolar level. In lingual view, the palate becomes higher at its posterior extremity (text-fig. 8D) as in MFT-K176. The distance separating the opening of posterior palatine foramen and the M^3 enamel-dentine contact is of 19.7 mm. The dimensions of MFT-K180 are presented in Table 2. The canine is represented by its incomplete root alveolus measuring 15.5 mm in its maximum buccolingual diameter. Premolars and molars are well preserved, slightly worn, displaying all details of their occlusal morphology. The postcanine tooth length (P^3–M^3) and premolar length (P^3–P^4) are nearly identical to those of MFT-K176.

P^3 crown has a sub-rectangular outline with a mesiodistal length on its buccal side slightly longer than on its lingual side. The parastyle is small and low and the paracone is distinctly higher than the protocone. The buccal and lingual walls of P^3 are slanted, the buccal wall being more slanted than the lingual. A preprotocrista joins the parastyle, delimiting a tiny and short anterior fovea near its buccal extremity. Two other crests issued from the protocone apex join the paracone and delimit a central fovea. A postprotocrista joins the posterior crest and ends at a tiny metastyle, delimiting a distal fovea. There is no trace of cingula, but on both buccal and lingual walls, there are several clear perikymata.

P^4 has a more rectangular outline than P^3 with a lingual mesiodistal length slightly longer than that of the buccal side. Both lingual and buccal walls are slanted. The parastyle and metastyle are present but weak and low. The protocone is mesially located and connected to the paracone by three crests, the anterior one delimiting a short and tiny anterior fovea. The central fovea is narrow. Two more small crests are issued from the protocone and are oriented distobuccally. They delimit a small distolingual fossette that may evolve as a distal wear facet. The paracone is slightly higher than the protocone.

Molars are high-crowned (crown height increasing from 7.35, 8.53, 8.95 mm at the paracone level from M^1 to M^3) and devoid of any cingula. The occlusal surface increases from M^1 to M^3 (M^1 represents 88 % of M^2 and M^2 represents 92 % of M^3). All molars have slanted lingual and buccal walls and display acute paracone and metacone cusps and sharp and elevated cristae obliqua. Their occlusal surfaces display coarse enamel wrinkles. M^1 is slightly worn, displaying a tiny dentine pit on the apex of its paracone and a slightly larger one on its protocone. Its crown is rather elevated, especially when compared to its width (57 %). Its occlusal surface has high relief with high paracone and metacone and distinct crista obliqua. The paracone and metacone apices are bent lingually, reducing the trigon surface. The metacone is slightly higher than the paracone. The anterior fovea is shallow, short and

located buccally. The crista obliqua is at an angle of 40° to the preprotocrista-hypoparacrista crest. Its MD length/BL width ratio is 88 % (Table 4). M^2 is larger and less worn than M^1 but still displays some wear facets on the protocone and the hypocone. Its buccal and lingual walls are slanted. The apices of the paracone and metacone are more salient than on M^1 and the trigon basin is deeper than on M^1. The main cusps are high. The crista obliqua is sharp, rather elevated, and is at an angle of 45° with the protocrista. A short and low crest joins the protocone and the hypocone. A short and shallow anterior fovea is present but is located buccally. The M^2 MD length/BL width ratio is 80%. M^3 is the largest tooth. Its occlusal surface, like that of M^2, does not show any dentine pits and only a few wear facets. Like P^4 and the other molars, its occlusal surface displays many coarse enamel crenulations that appear as vertically oriented enamel ridges on its lingual wall, as on M^1 and M^2. Its buccal and lingual walls are slanted, reducing the trigon surface with respect to the occlusal surface. Its hypocone is made of five distinct small cusplets connected to the postprotocrista. The small metacone is lower than the paracone so that the occlusal surface is reduced distally. A small additional cusplet is developed between the metacone and the hypocone complex. The enamel thickness measured on M^2 falls into "thick category" based on Martin (1985), similar to MFT-K176, both being thicker than that of the *K. piriyai* holotype (TF 6223) (Table 6).

From the µCT images, P^3 has three roots, two small buccal and one thick lingual root. The mesiobuccal root is curved lingually following the canine root curvature and the distobuccal root is the smallest one. P^4 has similar root characters as P^3 but the lingual root is more curved lingually and the mesiobuccal root is less thick than on P^3. The lingual root of M^1 is flattened and grooved; the buccal roots are flattened and grooved with bifid apices like those of M^2 and M^3. The distobuccal root of M^3 is missing (text-fig. 9).

Comparison and taxonomic assignment

Mandibles MFT-K177 and MFT-K181

Comparison with *Khoratpithecus*

MFT-K177 shares several characters with *K. piriyai* (TF 6223, holotype; CHAIMANEE et al., 2004), including the symphysis main structure and orientation, the lack of anterior digastric muscles scars, the structure of the P_4 and molars, and the high crown height of premolars and molars. They also have similar dental dimension (text-figs. 10A, 10B). The coronal sections of MFT-K177 are more massive, and the lateral eminence at M_3 level is more prominent than in TF 6223. Both share similar U-shape sections with vertical lateral flanges at the P_3–P_4 boundary level and similar sections at the M_3 level. The symphysis of MFT-K177 is similar to that of TF 6223 in its structure (text-fig. 4), but appears to be more massive, thicker and more extended distally until the distal level of M_1 instead of the mesial level of M_1 in TF 6223. The symphyseal inclination angles of both specimens are similar (40° in MFT-K177; 42° in TF 6223). However, several differences can also be observed. The tooth rows are posteriorly divergent in MFT-K177 rather than concave buccally as in TF 6223. This difference is related to the narrower anterior part of the mandible of MFT-K177. The intercanine breadth is smaller in MFT-K177 (18.71 mm) than in TF 6223 (31.35 mm) and its ratio between intercanine breadth and M_2 mesiodistal length is lower (1.37 in MFT-K177 and 2.27 in TF 6223). The maximum breadth measured between the buccal walls of left and right M_3 is wider on MFT-K177 (68.98 mm) than on TF 6233 (58.49 mm). The canines and incisors root alveoli are more vertical than those of TF 6223, on which the lingual walls of canine and incisor roots are more oblique and the roots more anteriorly oriented. The P_3 metaconid is smaller on TF 6223, inducing a concave lingual wall on this premolar in occlusal view, which appears to be convex on MFT-K177. There are high similarities between the teeth of these two hominoids, especially concerning P_4 and M_1. However, the M_3 occlusal surface of MFT-K177 represents 105 % of that of M_2, but this ratio is much larger in TF 6223 (140 %).

MFT-K181 is very similar and shares several characters with *K. piriyai* (TF 6223), including the lack of anterior digastric muscle scars. Its P_3 is larger. It has a larger buccolingually canine root diameter and a slightly longer P_3–M_3 length. Its jaw is more robust as attested by its higher elevation and stronger corpus. Its symphysis is thicker and extends more distally than in TF 6233, but it shares similar symphyseal inclination and structure with a thicker superior than inferior transverse tori and a weak genioglossal fossa. In lateral view, both share a similar post C–P_3 depression, a mental foramen under P_3 and wider buccinator grooves. It also displays some differences whose significance need to be assessed. The M_3 of MFT-K181 is less enlarged compared to its M_2 occlusal area, but this character is highly variable among hominoids as shown on *Sivapithecus* (BROWN 1989). The incisor roots and the labial alveolar upper part of symphysis are less inclined in MFT-K181. The incisor alveoli are narrower and their interalveolar septa thinner than in TF 6223. We could estimate the intercanine breadth (by doubling the value of the left corpus) as being approximately 18.3 mm instead of 31.35 mm in TF 6223. Therefore, if we consider that MFT-K181 belongs to the same species, according to its overall similarity with TF 6223, we have to consider that the intercanine breadth of *K. piriyai* mandibles display a large variation, from narrow with subvertical incisors (MFT-K181) to wide with proclined incisors (TF 6223). MFT-K181 shares most of its characters with the holotype of *K. piriyai*, from which it differs by its less proclined incisor alveoli, reduced intercanine breadth and smaller incisor alveoli. Its more robust corpus and larger canine alveolus suggest that it belonged to a more robust adult male individual, which was slightly younger than TF 6223.

MFT-K177 reveals several differences with *K. ayeyarwadyensis* (MFI-K171, holotype; JAEGER et al. 2011). The corpus of MFT-K177 is thicker and progressively deeper from the symphysis to M_3 instead of a nearly constant elevation in MFI-K171. Both share a similar symphyseal outline, but MFT-K177 displays a longer extension, until the distal level

of M_1 instead of the P_4/M_1 level, and a lower symphyseal inclination angle (40° in MFT-K177; 48° in MFI-K171). Its lateral eminences are more strongly developed than those of MFI-K171. The tooth row (P_3-M_3) of MFT-K177 is slightly longer (110 %) than that of MFI-K171. The P_3 of MFT-K177 is buccolingually wider and mesiodistally shorter than in MFI-K171. It develops a metaconid, which is not present in MFI-K171 and that displays a stronger parastylid. The P_4 is distinctly larger in length and width and develops a larger trigonid. A distinct anterior fovea on P_4 is not present in MFT-K177 but is well developed in MFI-171. The molar occlusal surfaces are similar but differ by their larger buccolingual dimensions and more elevated crowns. The M_3 occlusal surface is larger than M_2 (105 % in MFT-K177; 89 % in MFI-171), confirming the large variation of M_3 size on hominoids.

MFT-K181 displays several similar characters with *K. ayeyarwadyensis* (MFI-K171) but it differs by its larger size and higher elevation of molar crowns, larger canine alveoli and thicker mandibular corpus. The symphysis extends to the distal level of M_1 in MFT-K181 and to the P_4/M_1 level in MFI-K171. However, the symphyseal structure and inclination are similar.

Comparison with *Lufengpithecus*

We compared MFT-K177 with *Lufengpithecus lufengensis* (XU et al. 1978), the youngest *Lufengpithecus* (6.9 and 6.2 Ma; YUE & ZHANG 2006) on the basis of two well-preserved jaws, PA 548 and PA 580. MFT-K177 reveals several differences with *L. lufengensis*, including the less vertical and longer symphysis structure with a shorter inferior transverse torus. Anterior digastric muscles scars are absent in MFT-K177 but most of *L. lufengensis* specimens display these scars (XU & LU 2008). The lateral part of mandibular corpus elevation of MFT-K177 increases from P_3 to M_3, which is the opposite from *L. lufengensis*. The premolars and molars of *L. lufengensis* display very fine enamel wrinkles as in *Pongo*, but significant differences between the wrinkling structures of these both taxa have

been noticed (WARD 1997). MFT-K177 displays coarser enamel wrinkles, as in TF 6223 which are especially preserved on the crown surfaces of the little worn M_3 and on the talonids of right P_3 and P_4. The molars of MFT-K177 have vestigial mesial foveas, represented by tiny grooves, as in TF 6223, but *L. lufengensis* show larger mesial and central fovea. *L. lufengensis* P_3 have a triangular outline, oriented obliquely relative to the tooth row, their metaconid being located more distally to the protoconid, with longer mesiolingual cingulids and their talonids are much more developed than in MFT-K177. However, some P_3 specimen of *L. lufengensis* (PA 674.57) display a similar outline, but with a more distally located metaconid and a larger and more elongated talonid basin. MFT-K177 exhibits a wide mesial P_4 and a narrow and shallow talonid basin while the P_4 of *L. lufengensis* is narrow mesially and displays a deep talonid basin expanded distolingually. In addition, the anterior fovea of P_4 of MFT-K177 is reduced to a tiny groove, whereas it is well developed in *L. lufengensis*. Molars of male *L. lufengensis* display distinct anterior fovea, deep and large central fovea and less peripheralized cusps than those of MFT-K177 and *Sivapithecus* (WARD 1997). Their molar crown height is moderate when compared to those of MFT-K177.

Lufengpithecus hudienensis ZHANG et al. (1987) (8.2 and 7.1 Ma; YUE & ZHANG 2006) is less well documented than *L. lufengensis*. However, its tooth morphology is similar to that of *L. lufengensis* (ZHENG 2006), with a smaller size and thinner enamel. Their M_3 occlusal surface represent 102% of those of M_2. MFT-K177 displays the same differences in tooth morphology with *L. hudienensis* as those observed with *L. lufengensis.*

Lufengpithecus keiyuanensis WOO (1957) is the oldest *Lufengpithecus* species (12.5 – 11.6 Ma; LI et al. 2015). MFT-K177 has a longer P_3–M_3 length (67.16 mm) than *L. keiyuanensis* (58.5 mm) and its teeth do not display any cingulid. *L. keiyuanensis* exhibits stronger cusp relief with deeper grooves separating the cusps. P_4 to M_3 display wider and deeper anterior foveae. The P_3 is smaller and more mesiodistally oriented and shows no

metaconid. MFT-K177 displays a larger P_4 and its protoconid is larger than the metaconid with a slanted protoconid, whereas *L. keiyuanensis* has a smaller P_4, its protoconid is similar in size to the metaconid and its protoconid is not slanted. Its P_4 trigonid elevation is higher. The molars have a similar structure, but their cusps are proportionally more elevated than those of MFT-K177 and their central foveae are deeper. The buccal grooves separating trigonids from talonids are deeper and more strongly marked in *L. keiyuanensi* and its M_3 occlusal surfaces represent 104% of those of M_2, similar to MFT-K177. In general, this species is dentally very similar to that of *L. hudienensis* and according to the high variation observed on hominoid teeth, both taxa may be considered as conspecific.

Comparison with *Sivapithecus*

The mandible of MFT-K177 displays several characters distinct from *Sivapithecus* including the lack of anterior digastric muscle scars, the progressive elevation of the lateral part of mandibular corpus from the canine to M_3, the stronger development of the lateral eminence and the longer and less inclined symphyseal structure with a less enlarged superior transverse torus relative to the inferior transverse torus. MFT-K177 also displays larger molar occlusal surfaces than *Sivapithecus*. MFT-K177 differs from *S. sivalensis* (GSP 15000 and GSP 9564) by the absence of a post canine-P_3 fossa and the position of the mental foramen, which opens under the mesial level of P_3 root in MFT-K177, but in a more posterior position in GSP 15000. The latter also displays a larger but narrower P_3 with a stronger parastylid and lack of metaconid, and a smaller P_4 than MFT-K177. Molar crowns of MFT-K177, especially their lingual walls, are higher than those of *Sivapithecus*, at the same stage of wear, which appears clearly when compared with GSP 16082. MFT-K177 is more similar to *S. parvada* (BSPhG 1939 X4; KELLEY 1988), the largest species of *Sivapithecus*, both genera sharing robust mandibles with a strong lateral eminence at the M_3 level and wide buccinators grooves. However, *S. parvada* displays the highest lateral part of mandibular corpus elevation at the

symphysis level, not at the M_3 level. Its premolar and molar dimensions are larger than the corresponding teeth in MFT-K177.

Comparison with *Indopithecus*

Indopithecus giganteus (PILGRIM 1915) is approximately of the same geological age (8.85–8.60 Ma; PILLANS et al. 2005) as MFT-K177. Its mandible (CYP 359/68; SIMONS and CHOPRA 1969) is significantly larger than that of MFT-K177 in corpus and dental dimensions (text-figs. 10A, 10B). Both share robust jaws with massive and large lateral eminences, very long and thick symphyses reaching the distal level of M_1, and they lack post canine-P_3 depressions. Their lateral parts of mandibular corpus start to increase in thickness at the distal P_3 level and their ascending ramus hides the distal half of the M_3. They also share a wide and shallow buccinator groove at their alveolar plane. Despite size differences, MFT-K177 has a wider intercanine breadth (18.71 mm) than that of *I. giganteus* (13.60 mm) and the ratio between its intercanine breadth and M_2 mesiodistal length is higher (1.37 in MFT-K177 and 0.73 in CYP 359/68). Their P_3 are similar, sharing an oblique position relative to the tooth row, a strong metaconid slightly distal to the protoconid, a reduced parastylid and a reduced and narrow talonid basin. The P_4 are also similar in their organization, with a wide trigonid, a narrow talonid and a weak difference in elevation between the trigonid and the talonid. The molars share the dryopithecine pattern, but those of *I. giganteus* display more elongated crowns, their MD length/BL width ratio being higher than those of MFT-K177 (Table 4). The elevation of molar crowns in MFT-K177 is similar to that of *I. giganteus*, whereas the breadths of *I. giganteus* molars are considerably larger. Therefore, despite high superficial resemblance the two taxa differ fundamentally by the presence of anterior digastric muscles scars in *I. giganteus* and the less inclined symphysis (40° in MFT-K177; 64° in CYP 359/68), the narrower anterior dentition and more reduced canines of *I. giganteus*, which is considered to be a close relative of *Sivapithecus* (BEGUN 2015).

Comparison with *Ankarapithecus*

Ankarapithecus meteai Ozansoy, 1965, from the late Miocene of Turkey (9.8–9.6 Ma; KAPPELMAN 2003) is supposed to be the most basal known member of the pongine clade (BEGUN & GÜLEC 1998; BEGUN 2015). *Ankarapithecus meteai* differs from MFT-K177 by the more vertical orientation and section outline of its symphysis and by the occurrence of impressions of anterior digastric muscles on the inferior lingual surface of the symphysis (KAPPELMAN 2003). The mandibles are represented by two samples, a small one attributed to a female AS95-500 (ALGAPUT et al. 1996) and a large one attributed to a male MTA 2125 (OZANSOY 1965). The female symphysis (AS95-500), which is complete, shows a strong superior transverse torus and a narrow, posteriorly elongated inferior transverse torus, quite different from that of MFT-K177. The tooth rows of AS95-500 are also moderately divergent and display similar intercanine breadth, and both taxa display vertically oriented incisors. The male specimen (MTA 2125) tooth row differs from that of MFT-K177 by the large increase of size from M_1 to M_2 and by its M_3 smaller than M_2. The elevation of the crowns is also lower than in MFT-K177.

Comparison with *Pongo*

Pongo has larger jaws and teeth and displays a much less robust masticatory apparatus, a wider and more anteriorly extensive incisal area and larger and more proclined incisors. The highest elevation of the corpus is located at the symphysis level rather than at M_3, and the posterior part of the mandible is buccolingually very narrow compared to the large lateral eminences developed on MFT-K177. Symphyses of *Pongo* are less inclined and differ by the shape of their section (JAEGER et al. 2011) which is thinner, shows a deeper genioglossal fossa with a thin and more distally extended inferior transverse torus (simian shelf) (BROWN 1997). *Pongo* displays a U-shaped dental arcade, and its tooth rows tend to converge distally. A distinct diastema is present between the canine and the P_3 in *Pongo*, but

it is absent in MFT-K177. The P_3 of *Pongo* is proportionally larger than that of MFT-K177. It has a smaller metaconid, a stronger parastylid and a wider talonid basin. The P_4 of *Pongo* is more buccolingually developed and its talonid basin is larger and wider. The enamel surface of *Pongo* molars displays numerous tiny wrinkles that are absent in MFT-K177. TAYLOR (2006) has compared metric data of *K. piriyai* (TF 6223) with those of extant *Pongo*, concluding that "with the exception of relatively thicker M_3 mandibular corpus, it displayed jaw proportions that would be expected for an extant orangutan of comparable jaw size". We therefore compared MFT-K177 to the same set of data provided by Taylor (2006) and observed similar results. In addition to thicker mandibular corpus at M_3 level, MFT-K177 displays a higher M_3 corpus depth that falls outside the variation of extant orangutans. The symphyseal measurements also fall within the orangutan range to the exclusion of its inclination, the angle of which falls clearly outside the range of orangutan variation and even of that of gorilla (JAEGER et al. 2011). Therefore, it appears that MFT-K177 is already specialized in a direction that is distinct from that of *Pongo* and similar to that of *Indopithecus*.

The mandible MFT-K181, as the holotype, differs from *Pongo* by its more robust mandibular corpus, its narrower intercanine breadth and its less flattened and less posteriorly extended inferior transverse torus (simian shelf). The symphyseal angulation is also lower than in *Pongo* (JAEGER et al. 2011) and the incisors roots are less proclined. The mental foramen, located under the anterior root of P_3 in MFT-K181, is situated more distally (under P_4) in *Pongo.* The talonid of P_4 is smaller and buccolingually less extended than that of *Pongo*. We have introduced the values of MFT-K181 in Taylor (2006) comparison, which confirm the previous observation but also display additional differences. MFT-K181 falls clearly outside the *Pongo* range for M_3 corpus depth in addition to M_3 corpus thickness as in

MFT-K177. P_4 and molars mesiodistal measurements fall, as those of TF 6223, within the *Pongo* range including its M_3, which are near the upper range values of *Pongo*.

Taxonomic assignment

MFT-K177 is a mandible fragment that shares several similar derived characters with *K. piriyai* (TF 6223) including the lack of anterior digastric muscle scars, the symphyseal inclination angle and section outline, the tooth dimensions and occlusal surface organization, the lack of cingulids on premolars and molars and the similarity of the mandibular corpus transverse sections. However, it differs from TF 6223 by a narrower intercanine breadth, lower elevation of the jaw at the P_3–P_4 level, a higher robusticity of the mandibular corpus at P_4 and M_1, a posteriorly extended symphysis, the lack of a post canine-P_3 depression, a more developed metaconid on P_3, and a more vertical orientation of the lingual root walls of incisors and canines. According to the previous list of *Khoratpithecus* characters that are all shared with MFT-K177, we assign it to *K. piriyai* CHAIMANEE et al. (2004). Its general resemblance to TF 6223 suggests that it could be attributed to an older male individual of that species because of the greater wear of its teeth, its more robust jaw, with thicker and more distally extended symphysis and the higher robusticity index of its corpus. However, several important differences have to be interpreted as high individual variation within this species. Among them, significant anatomical differences include the divergent shape of the tooth rows, the narrow intercanine breadth, the low elevation of the anterior part of the corpus versus the posterior part, the more vertical position of the incisor and canine alveoli, the absence of post C-P_3 depression, the thicker and more distally extended symphysis and the higher corpus elevation at the M_3 level. At P_3 level, TF 6223 is significantly wider. The distance between M_3 is larger in MFT-K177 because of the stronger divergence of the tooth rows. Nevertheless, if the variation observed among *Sivapithecus* and *Lufengpithecus* specimens is taken into account, these differences can be considered as being compatible with

intraspecific variation. One additional peculiar point of MFT-K177 concerns its strong asymmetry, which is indicated by its tooth wear, the different thickness of the lateral eminences at the M_3 level, the different widths of its left and right buccinator grooves and by its distinct M_3 widths. MFT-K177 also shares several characters with *I. giganteus:* large size, massive mandible with high robusticity index that increases in height posteriorly, strong lateral eminences and wide buccinator grooves, symphysis extended to the distal M_1 level, lack of post C-P_3 depression, strong metaconid on P_3, reduced intercanine breadth and canines vertically implanted. These characters might suggest close phylogenetic relationships between these two species. Nevertheless, many important differences can be observed, including the occurrence of anterior digastric muscle scars in *I. giganteus*, its larger size, more vertical symphyseal inclination with different section outline, more reduced breadth across the incisor area, larger P_3 metaconid, less elevated molar crowns with distinct MD length/BL width proportions, vertical buccal premolar and molar walls and less divergent tooth rows. Based on these differences, we consider that some of them are related to the high robusticity of both mandibles and others to a similar dietary adaptation so that most of these similarities may be attributed to homoplasy. We therefore attribute this mandible to *K. piriyai*, despite the differences observed with the holotype mandible. These differences are attributed to a greater individual age for this individual, also presumed to be a more robust adult male, and to individual variation.

MFT-K181 displays most of the mandibular and dental characters that define the genus *Khoratpithecus* such as the lack of anterior digastric muscle scars, superior transverse torus thicker than the inferior one, low inclination of the symphysis in relation to the alveolar plane, long symphysis extending to M_1 level, the high robusticity index of the mandibular corpus, position of the mental foramen under the anterior root apex of P_3, posterolingual root of P_3 oriented lingually not in line with the other premolar and molar roots, reduction of

anterior fovea, coarsely wrinkled enamel, lack of cingulids and strongly slanted buccal walls on premolars and molars, vertical lingual walls with sharp post-metaconid and pre-entoconid crests on molars. MFT-K181 displays anatomical characters and dimensions that are highly similar with those of *K. piriyai* (TF 6223) (Table 2– 5). It differs in only a few characters, including a larger canine alveolus, a smaller M_3, thicker enamel, and narrower intercanine breadth. The last character is important, because it demonstrates the variability of the anterior jaw width in *K. piriyai* (narrow in MFT-K181 and MFT-K177; very wide in TF 6223). Therefore, we assign also MFT-K181 to *K. piriyai* CHAIMANEE et al. (2004).

Maxilla MFT-K180

Comparison with MFT-K176

The maxilla of MFT-K180 displays unworn premolars and molars and thus contributes to the knowledge of the upper dental morphology of this genus. MFT-K180 is very similar to MFT-K176 (CHAIMANEE et al. 2019) in morphology. Very few differences, however, can be observed between these two specimens, among which are a deeper postcanine fossa on MFT-K180 and a greater palatine foramen that does not extend beyond the posterior level of M^3 crowns as on MFT-K176. Their premolars and molars display several characters that have led CHAIMANEE et al. (2019) to suggest that the MFT-K176 maxilla could belong to cf. *Khoratpithecus* and the characters of MFT-K180 strongly support this attribution. All upper molar characters of *Khoratpithecus* (CHAIMANEE et al., 2003) are present on this new specimen (MFT-K180). The P^3 is rather rectangular in its occlusal outline with a weak parastyle and it does not displays an anteriorly expanded parastyle area. Its lingual and buccal walls are slanted, like those of P^4, which is mesiodistally longer lingually than buccally. The ratio of P^4 area to M^1 area are similar (0.61 in MFT-K180 and 0.62 in MFT-K176). The molars are wider buccolingually than mesiodistally (text-figs. 10C, 10D), even though the MD length/BL width ratio of MFT-K176 has been exaggerated by the strong oblique wear of

the M^1 (75%) and M2 (79%). They also display a less open trigon angle than other genera. Both specimens have slanted buccal and lingual walls on the molars, coarse enamel wrinkles and elevated cristae obliqua. Some differences can be observed between the two maxillae that are related to their different stage of wear. The strong buccolingual versus mesiodistal length ratio of M^1 of MFT-K176, which appears clearly related to the strongly oblique wear of this tooth and its very low trigon angle might correspond to individual variation.

Comparisons with *Khoratpithecus chiangmuanensis*

Only a few upper teeth (P^3, M^2 and M^3) of *K. chiangmuanensis* (CHAIMANEE et al. 2003) can be compared with MFT-K180. The P^3 of *K. chiangmuanensis* (TF 6175, female) shares a similar occlusal outline, cusp organization and lack of cingula, and differs by the weaker development of the transverse crests issued from the protocone delimiting the central fovea. The upper M^2 (TF 6169 male; TF 6176 female) of *K. chiangmuanensis* are also very similar in size and morphology. MFT-K180 shares *Khoratpithecus* characters, like the crenulated enamel, the lack of cingula, the large hypocone, the large posterior fovea, the sharp and elevated crista obliqua, and the slanted buccal and lingual walls. The M^2 of *K. chiangmuanensis* differ in their MD length/BL width ratio, which reaches values of 94% (TF 6169) and 95% (TF 6176) but only 80% for MFT-K180, indicating a greater molar relative width of MFT-K180. The M^3 (TF 6177 female) is smaller than M^2, unlike that of MFT-K180 in which M^3 is larger than M^2, but both share a similar MD length/BL width ratio (87% in TF 6177; 89% in MFT-K180).

Comparisons with *Khoratpithecus* sp. from Myanmar

The isolated upper M^2 of *Khoratpithecus* sp. (MFI 89) from the late Miocene of Myanmar (JAEGER et al. 2011) displays striking similarities with the M^2 of MFT-K180. Both share a high crown, wrinkled enamel, and similar cusp organization, as listed above. However, they differ by their ML length/BL width ratio, which is 98% for MFI-89, indicating

a nearly square outline. Therefore, comparison with other known *Khoratpithecus* upper molars suggests a great homogeneity of their characteristics, except for crown proportions, which seem to represent a diagnostic character of *K. piriyai*.

Taxonomic assignment

MFT-K180 is a new hemi-maxilla which displays strong similarities with MFT-K-176 in its dentition and maxillary morphologies and dimensions (Table 2 and 4). Due to its unworn premolars and molars, it provides important additional information concerning occlusal structure and the M^1 MD length/BL width proportions, which were obscured in MFT-K176 by its strongly oblique wear. MFT-K180 displays several upper teeth characters that are diagnostic of *Khoratpithecus* (CHAIMANEE et al. 2003; JAEGER et al. 2011), including the absence of cingula on the premolars and molars, the coarse enamel wrinkling, the slanted buccal and lingual walls of the premolars and molars, the molar MD length/BL width proportions and the sharp crista obliqua of the molars. It differs from MFT-K176 only in having a larger M^3 and a slightly deeper canine fossa. According to its strong similarities with MFT-K176 and the high resemblance of both maxilla fragments to the holotype mandible, we assign MFT-K180 and MFT-K176 to *K. piriyai* CHAIMANEE et al. (2004).

Khoratpithecus magnus n. sp.

(text-figs. 11–12)

Type specimen: MFT-K178, mandible fragment with well-preserved left P_4–M_2, alveoli of C and P_3 and root of right P_4, housed in Chulalongkorn University, Bangkok.

Locality and age: Khorat sand pit, Nakhon Ratchasima Province, northeastern Thailand, late Miocene, between 9 and 6 Ma.

Etymology: species name refers to its large size.

Diagnosis: Species of *Khoratpithecus,* significantly larger than *K. piriyai,* with an estimated body mass of about 74 kg, characterized by its larger dental size, large and high crowned P_4 and molars. Rectangular M_1 and M_2 crowns with high dental proportions (MD length/BL width) of 119% and 128% respectively. Symphysis with a very thick superior transverse torus and a deep genioglossal fossa. Narrow anterior mandible with a reduced intercanine breadth.

Differs from *K. piriyai* (TF 6223) by the higher crown of its P_4, M_1 and M_2, the verticality of the buccal walls of P_4 and lower molars and the MD length/ BL width proportions of M_1 and M_2, its thicker enamel, the greater thickness of its superior transverse torus, the deep genioglossal fossa and the more distally extended symphysis. Differs from *K. ayeyarwadyensis* (MFI-K171) by most of the same characters as from *K. piriyai*. Differs from *K. chiangmuanensis* by its larger dental size, even from the male specimens, the more vertical buccal walls of lower molars, higher molar crowns, more molarized P_4 and its higher molar MD length/BL width ratios and flatter occlusal surfaces.

Dimensions: Tables 2–5.

Description:

MFT-K178 is a fragment of mandible that preserves parts of the symphysis, left P_4 to M_2 and roots of right P_4. The anterior part of the jaw is broken away, leaving visible only the lingual walls of the canine alveoli and both P_3 distal root alveoli. The left horizontal ramus is broken obliquely at a level behind M_2 and the right one is broken behind P_4 roots. In lateral view, the left lateral part of the mandibular corpus displays elevated P_4-M_2 crowns and a high elevation of the corpus under P_4 (41.80 mm). In inferior view, the narrowness of the anterior part of the jaw is indicated by the short distance separating the right and left mental foramina (29.70 mm). These mental foramina open about 28.71 mm below the alveolar level, under the apex of the anterobuccal root of P_3. In addition, a short post canine-P_3 fossa is developed under P_4. The symphysis is broken anteriorly and posteriorly but displays a deep and well-

excavated genioglossal fossa located below a very strong and thick superior transverse torus (28.75 mm). The inferior transverse torus is much thinner (13.75 mm) and extended posteriorly but its length cannot be estimated precisely, although it reached at least the distal level of M_1. The symphyseal inclination angle is about 40 ° with the alveolar margin. The inferior part of the mandible is missing and therefore the anterior digastric muscles scars cannot be observed (text-fig. 11B).

The incisor area is missing. The maximum diameter of the canine alveoli is of 14.5 mm and they are located close to each other, the intercanine breadth measuring 17.86 mm. The canine alveoli are deep, they reach the basis of the mandibular corpus and have an oval outline, being oriented obliquely in the jaw. P_3 distal roots are only represented by their sockets. The unworn left P_4 has a nearly square occlusal surface, being slightly wider buccolingually than mesiodistally. Its trigonid is wider than the talonid and occupies most of the occlusal surface, with the protoconid higher than the metaconid, both cusps being separated by a longitudinal groove that connects the mesial fovea to the talonid basin. The mesial fovea is broad and relatively shallow with wrinkled enamel. The talonid is deeper with strongly wrinkled enamel. Postprotocristid and postmetacristid are well developed and extend distally to three low rounded tubercles, which are located lingually to one small hypoconid cusplet developed on the elevated distal marginal crest. The P_4 displays a vertical and high crown (11.2 mm above the enamel-dentine contact), with a crown height index of 94 % (H/BL=11.2/11.89).

The molars of MFT-K178 differ from those of other specimens from this locality by their larger size (Table 2), higher crowns and higher dental proportions (Table 4). The M_1 displays a high crown with a crown height index of 81 % (H/BL=9.67/12.00) and is elongated (MD length/BL breadth ratio 119 %; Table 4). It is characterized by the large distance separating the protoconid from the hypoconid and by its vertical buccal and lingual crown

walls. An additional cusplet also develops on the post-metacristid, which is well separated from the metaconid and the pre-entocristid, especially on M_1. However, several tooth characters are similar to the other specimens described here, such as the reduced anterior fovea, the sharp and rectilinear crest made from the connection between the pre-entocristid and the post-metacristid and the absence of cingulids. The M_2 is significantly larger than M_1 with a larger MD length/BL breadth ratio (128%) and a similarly rectangular crown outline. Its crown displays many enamel wrinkles and a deeper talonid basin. The distal fovea is also larger and the post-metacristid and the pre-entocristid constitute a sharp crest that lines the lingual border of the crown. The entoconid is more reduced compared to the hypoconid than on M_1. There is no interstitial contact facet on the distal wall of this molar. According to its large size, we have suspected that it might represent an M_3, but detailed investigation using µCT images from multiple sections have confirmed that it corresponds to the M_2 of this specimen. On the right lateral part of mandibular corpus fragment, only the P_4 is present but its crown is broken at the enamel–dentine level. The enamel thickness measured on M_2 falls into "thick category" based on Martin (1985). It displays the thickest enamel among *Khoratpithecus* specimens (Table 6). Based on µCT images, the P_4 has two mesial and distal roots, which are rather long, and the tips of the roots are split into two. The molars have two long mesial and distal roots which are divided into two at their apices. The M_2 roots are as long as those of M_1 but larger (text-fig. 12).

Comparison and taxonomic assignment

Comparison with *Khoratpithecus*

MFT-K178 differs by several characters from *K. piriyai* (TF 6223 holotype; CHAIMANEE et al., 2004). The intercanine breadth is much narrower in MFT-K178 (17.86 mm) than in TF 6223 (31.35 mm). Therefore, the ratios between intercanine breadth and M_2 mesiodistal length are very distinct (0.98 for MFT-K178 and 2.27 for TF 6223). MFT-K178

has significantly larger teeth, concerning not only their occlusal surface, but also their crown height. P_4 and molar sizes are not correlated to an increased size of the canine alveoli. The buccal crown wall of P_4 in MFT-K178 is vertical whereas it is bent lingually in TF 6223 and MFT-K177. The dental proportions of M_1 and M_2 of MFT-K178 (119 % and 128 %) are higher than in TF 6223 (115 % and 108 %) (Table 4). Another difference concerns the relations between metaconid and entoconid. In MFT-K178 there is a cusplet, located distal to metaconid, and separating the post-metacristid from the pre-entocristid. This cusplet is strongly developed on M_1, and more reduced but still distinct on M_2. The nearly continuous and sharp lingual crest (post-metacristid + pre-entocristid) connecting the metaconid and the entoconid is therefore less sharp than in TF 6223.

On a virtual µCT image of the symphysis section, the thickness of the superior transverse torus appears to be much larger than in other specimen of *K. piriyai* (text-fig. 4) and the genioglossal fossa is more deeply excavated. The slope of the planum alveolae is also less steep. Therefore, MFT-K178 presents a mixture of *Khoratpithecus* characters, as the tooth morphology, the symphyseal inclination angle, the location of mental foramina, but it differs significantly from TF 6223 by its narrower intercanine breadth, thicker symphysis with stronger superior transverse torus, deeper genioglossal fossa, larger P_4 and molars, distinct dental proportions and crown height.

The mandible MFT-K178 shares some characters with that of *K. piriyai* (MFT-K177), including a narrow intercanine breadth, small canine alveoli, and similar distance between the left and right mental foramina (29.70 mm in MFT-K178 and 29.36 mm in MFT-K177). However, some characters distinguish both mandibles: the ratio between intercanine breadth and M_2 mesiodistal length (0.98 for MFT-K178 and 1.37 for MFT-K177), the higher elevation of the corpus at P_4 level (41.80 mm in MFT-K178 versus 35.5 mm in MFT-K177)

and the P_4 and molar sizes, proportions and crown heights which differ in the same way as with the molars of TF 6223.

Comparison with *Sivapithecus*

The dental dimensions of MFT-K178 are significatively larger than those of *S. indicus* and *S. sivalensis*. Therefore, we compared it with the largest species of *Sivapithecus*, *S. parvada* (KELLEY 1988). The differences concern the mandibular corpus, which is more massive in MFT-K178 than in *S. parvada*, with a thicker and higher corpus at the anterior part of the mandible. The symphyses differ significantly by their different orientation and their cross-sectional outline, the symphysis of all *Sivapithecus* species being more vertical (JAEGER et al. 2011). The canine alveoli of *S. parvada* are larger compared to those of MFT-K178. The P_4 and molar sizes are similar but the M_1 and M_2 crowns of MFT-K178 are mesiodistally longer. The MD length/BL width ratio of *S. parvada* molars are of about 104–107 %, indicating more square molar crowns (KELLEY 1988). The occlusal surfaces of *S. parvada* molars are flatter. The differences of their premolar and molar occlusal surfaces are similar to those already pinpointed between *Sivapithecus* and *Khoratpithecus* at the generic level (CHAIMANEE et al. 2006).

Comparison with *Indopithecus*

The lower jaw of *I. giganteus* (CYP 359/68; SIMONS & CHOPRA 1969) and MFT-K178 belong to very large apes of nearly the same size, albeit *I. giganteus* displays slightly larger dimensions of its postcanine teeth. In both specimens, the canines are of reduced size compared to molars and located close to each other. However, the intercanine breadth in *I. giganteus* is more reduced than in MFT-K178 (13.60 mm versus 17.86 mm) (Table 3) with a distinct ratio between intercanine breadth and M_2 mesiodistal length (0.73 versus 0.98). The P_4 of CYP 359/68 is larger and significantly wider buccolingually than that of MFT-K 178. Molar crowns MD length/BL width ratios of both taxa are rather similar on M_1 and M_2 (120

% and 119 % for CYP 359/68 versus 119% and 128 % for MFT-K178). However, their crown height are very different, the molar crowns of *I. giganteus* being much lower than those of MFT-K178, even if differences in wear are taken into account. The ratio between crown heights measured at the metaconid and maximal crown BL width are 46.5% for CYP 359/68 (SIMONS & CHOPRA 1969) and 81% for M_1 and 60 % for M_2 in MFT-K178. The occlusal surfaces are flat, and no enamel wrinkles are present on CYP 359/68. In lateral view, both corpora are elevated and massive but CYP 359/68 does not display a postcanine-P_3 fossa. The mental foramen of CYP 359/68 is located under P_4, 26 mm below the alveolar margin, at about the middle of the corpus height, whereas it is located at the basis of the symphysis and under the apex of the P_3 anterobuccal root in MFT-K178. In ventral view, the width measured at P_4 level is similar (51 mm for CYP 359/68; 52 mm for MFT-K178) and the symphyses maximal thickness are almost identical (28.4 mm for CYP 359/68; 28.75 mm for MFT-K178). However, their symphyseal sections differ in an important way, the symphyseal angle being more vertical: 64° in CYP 359/68 and 40° for MFT-K178. In addition, MFT-K178 displays a very thick superior transverse torus compared with the inferior transverse torus, whereas both tori exhibit nearly the same thickness in CYP 359/68. The inclination of the planum alveolare is low in MFT-K178, much stronger in CYP 359/68 and the genioglossal fossa is more deeply excavated in MFT-K178.

The isolated M_2 or M_3 of *I. giganteus* (GSI D-175, Pilgrim, 1915) well-illustrated by VON KOENIGWALD (1951) shows more resemblance to the M_2 of MFT-K178 than to those of CYP 359/68. Both share comparable coarse wrinkles and similar dental occlusal area (292 mm^2 for GSI D-175; 260 mm^2 for MFT-K178) and their MD length/BL width ratios are similar. Their crown organization is also comparable, differing mainly by the sharp and nearly continuous lingual crests in MFT-K178, which are interrupted by a deep groove separating the metaconid and the entoconid on GSI D-175. In addition, the protoconid is narrower

mesiodistally and deep grooves separate the buccal cusps in GSI D-175, which are connected on M_1 and M_2 of MPF-K178.

Despite such shared characters such as large size, the reduction of canines and the narrow intercanine breadth, several important differences, including symphyseal shape and orientation, the P_4 structure and the sharp and continuous lingual molar crests, do not support close relationships between these two taxa. Instead, we consider that the resemblances between these two large fossil apes correspond to a similar adaptation for feeding on hard or fibrous food.

Taxonomic assignment

The estimates body mass of MFT-K178 is about 74 kg, approximately 30% more than other *Khoratpithecus* individuals from the same locality (Table 8). It shares several characters with *Khoratpithecus*, including the inclination of its symphysis, the position of the mental foramen under the P_3 root, the P_3 distolingual root oriented orthogonally to the tooth row, the P_4 and molars with coarse enamel wrinkling, the absence of cingulids, and shallow mesial foveae. Nevertheless, it differs from other *Khoratpithecus* specimens by its larger size and higher elevation of P_4 and molar crowns, the verticality of the P_4 and molar buccal walls and by the MD length/BL width proportions of its molars. The thickness of the superior transverse torus of the symphysis and its deep genioglossal fossa are also significant. These differences cannot be attributed to sexual dimorphism because its canine alveoli are of the same size as those of *K. piriyai*. A comparison with *I. giganteus* also reveals several important differences, similar to those pinpointed for MFT-K177 that exclude phylogenetic proximity to that genus. Because the differences observed among other known mandibles of *Khoratpithecus* from the same geological unit are significantly larger than what can be accepted as intraspecific variation and sexual dimorphism (KELLEY & XU 1991), due to the small size of the canine alveoli, we propose to assign this mandible fragment to a new species, *Khoratpithecus*

magnus n. sp. It is also difficult to determine the sex of this individual because the canine alveoli are of the same size as on the other lower jaws described from the same locality but the P_4 and the molars are significantly larger.

Khoratpithecus sp.

(text-figs. 13, 14)

Specimen: MFT-K179, mandible fragment missing tooth crowns, only preserving roots of left C–M_1 and right C–M_2 with alveolar fragments of I_1 and I_2.

Locality and age: Khorat sand pit, Nakhon Ratchasima Province, northeastern Thailand, late Miocene, between 9 and 6 Ma.

Measurements of mandible: Tables 3, 5.

Description:

MFT-K179 represented a mandible fragment without tooth crown (text-fig. 13). The labial part of the anterior dentition is missing so that the alveoli and roots of the incisors are not preserved. The canine roots are preserved but broken under the cervical line. The intercanine breadth is reduced (15.47 mm). The length between the mesial root of P_3 to the distal root of M_2 is about 52.15 mm (compared with P_3–M_2, 46.57 mm for TF 6223, 50.32 mm for MFT-K177, 50.73 mm for MFT-K181 and 46.27 mm for MFI-K171). On the left corpus, which is broken behind a large hollow cavity corresponding to M_2 position and produced by a periodontal lesion, the distance between P_3 and M_1 measures 40.5 mm. The diameter of the left canine root measures 15.3 mm, in the range of the other fossil hominoid canine diameters from the same locality.

In lateral view, the jaw appears to be rather shallow, its height being 37.34 mm under the left M_1 (Table 5). A large mental foramen opens near the basis of the jaw, at the level of the contact between P_3/P_4 (text-fig. 13E). The distance between the left and right mental foramina is about 27.80 mm, indicating a narrow anterior part of the jaw compared to other

specimens from this locality. The symphysis is long, strongly inclined with an inclination angle of 43° and extends until the level of the distal crown of M_1 (text-fig. 13A). The inferior transverse torus is thinner (15.7 mm) than the superior transverse torus (24.0 mm) and the shallow genioglossal fossa displays three rounded foramina, two symmetric ones located on each side of the deepest part of the fossa and one sagittal, located 10 mm above (text-fig. 13D). Its basal part is well preserved and displays no trace of anterior digastric muscle scars (text-fig. 13B).

Based on μCT images, the canine roots are thick, deep and the apices of the roots point lingually (text-fig. 14). The distolingual root of P_3 is oriented lingually, being extended orthogonally to the tooth row. The P_4 has two roots, mesial and distal, which are rather long, and the tips of the roots are split into two. The molars have two long mesial and distal roots, which are divided into two at their apices.

Comparison and taxonomic assignment

MFT-K179 shares with *Khoratpithecus* the absence of anterior digastic muscle scar, the symphysis orientation and organization, the canine root diameters, and the organization of the premolar and molar roots. However, it differs from the holotype of *K. piriyai* (TF 6223) by the narrowness of the symphysis expressed by the reduced intercanine breadth, the reduced elevation of the anterior part of its corpus at P_4 level and the position of the mental foramen. Because of its incompleteness, this specimen cannot be assigned to a specific attribution. Therefore, it is provisionally referred here to cf. *Khoratpithecus* sp.

4. Discussion

Taxonomic assignment of MZKB-K-001

MZKB-K-001 corresponds to a left lower jaw fragment of a late Miocene hominoid from the Irrawaddy Formation in Myanmar, which was assigned to a Ponginae gen. et sp.

indet. by TAKAI et al. (2021). It originated from the Irrawaddy Formation and shares several morphological characters with *K. ayeyarwadyensis* (MFI-K171; JAEGER et al. 2011), including the shape of the dental arcade, the position of the mental foramen under P_3, the depression of the buccal jaw surface under P_4 to M_2, the same position and development of the mylohyoid line, the similar roots, the similar tooth dimensions and the lack of scars for the anterior digastric muscles. These characters constitute additional evidence to refer this jaw to *Khoratpithecus*. The main argument that led TAKAI et al. (2021) to propose MZKB-K-001 as a taxon distinct from *Khoratpithecus* was based mainly on the outline of the mandibular symphyseal section. However, the mandibular symphysis of MZKB-K-001 is incomplete, its upper part being missing, and its lower part does not display a section well oriented in the midsagittal plane. Therefore, some peculiarities like the supposedly deep genioglossal fossa and the strong bulging of the superior transverse torus of the symphysis can be interpreted as artifacts due to the irregular section. Its inferior transverse torus extends to the P_4/M_1 level as in *K. ayeyarwadyensis* (MFI-K171 Holotype; JAEGER et al. 2011). The inclination of the symphyseal section seems to be less inclined than in other known *Khoratpithecus* specimens, including those described here. However, the upper part of the mandibular symphysis is broken, precluding accurate measurement of this inclination angle. When compared with the new specimens of *Khoratpithecus* described here, the main morphological differences between *K. ayeyarwadyensis* and *K. piriyai* concern the mandibular corpus thickness at M_3 level, which is thinner in this individual and its relatively lower corpus robusticity index. We therefore tentatively refer MZKB-K-001 to *K.* cf. *ayeyarwadyensis*.

Character variation in *Khoratpithecus*

Mandibular shape and robustness

The dental arcade shape of the mandible is rather variable among *Khoratpithecus*. The holotype of *K. piriyai* (TF 6223) displays a wide intercanine breadth compared with the MD length of M_2 (2.27; Table 3) and an U-shaped dental arcade similar to that of *Pongo*. The new

specimens of *Khoratpithecus* (MFT-K177, K178, K179) have narrower intercanine breadth as in *Lufengpithecus* (ZHENG 2006), *Sivapithecus*, *Indopithecus* (SIMONS & CHOPRA 1969) and *Gigantopithecus* (ZHANG & HARRISON 2017). *Khoratpithecus piriyai* has a relatively thick mandibular corpus with the maximum thickness at the level of M_3, and a relatively high corpus robusticity index (66–78; Table 5). The mandibular corpus is roughly of the same height from P_3 to M_3 as in *Sivapithecus* except for MFT-K177, in which the mandibular corpus height increases posteriorly. To the contrary, *Lufengpithecus* displays a mandibular corpus height decreasing posteriorly (ZHENG 2006). The Myanmar hominoids, *K. ayeyarwadyensis* (MFI-K171) and *K.* cf. *ayeyarwadyensis* (MZKB-K-001) display thinner mandibular corpus with roughly the same height from P_3 to M_3 and a corpus robusticity index (59–64; Table 5) relatively lower than that of the Thai *Khoratpithecus*.

Mandibular symphyseal morphology

Most of the Khorat specimens are broken at the symphyseal area but their symphyseal lengths are rather long (approximately more than 47.5 up to 54.4 mm; Table 3). They have an inferior transverse torus that extends posteriorly to the distal part of M_1 as in *I. giganteus*, except the holotype of *K. piriyai* (TF 6223) in which the inferior transverse torus extends to the mesial part of M_1. The Myanmar *K. ayeyarwadyensis* displays a shorter symphysis (34.81 mm) with the inferior transverse torus extending to P_4/M_1. In *Pongo* and *Gigantopithecus*, it extends to P_4 or M_1 (BROWN 1997; ZHANG & HARRISON 2017) and to M_1 in *S. parvada* (BROWN 1997). *Khoratpithecus* display thick symphyseal breadth at the superior transverse torus (21–25 mm), except *K. magnus* n. sp. (MFT-K178) which displays a larger value (28.75 mm) and *K. ayeyarwadyensis* (MFI-K171), which displays a thinner symphyseal breadth (17.33 mm; JAEGER et al., 2011). The symphyseal inclination angles of the Thai specimens of *Khoratpithecus* are of about 40–45°, which is slightly lower than in *K. ayeyarwadyensis* (48°;

JAEGER et al. 2011), and markedly lower than *Gigantopithecus* (51.5–59°; ZHANG & HARRISON 2017) and *Indopithecus* (64°; JAEGER et al. 2011) (Table 3).

Dental morphology and proportions

Khoratpithecus displays high variability in dental morphology and size (Table 2, 4). The P_3 displays an oblique orientation to the long axis with a longer MD length than a BL width (dental proportions range from 139–167 %), except MFT-K177 which exhibits equal dimensions. The P_4 shows nearly the same MD length and BL width (dental proportions range from 90–100 %), except *K. ayeyarwadyensis* (MFI-K171) that displays a shorter mesiodistal length than the buccolingual width (83 %). M_1 and M_2 have MD length longer than BL width (dental proportions range from 104–128 %). However, all M_3 are significantly longer mesiodistally than buccolingually (dental proportions range from 122–134 %).

The upper premolars and molars of *K. piriyai* (MFT-K180) display similar dental proportions to those of *Sivapithecus*, but *K. piriyai* (MFT-K176) molars are narrower mesiodistally than buccolingually, differing from *Pongo*, which displays nearly square molars and broader premolars.

Dental enamel thickness

The relative enamel thickness of Khorat hominoids reflects high variation (Table 6), most of them falling into the "thick" enamel category defined by MARTIN (1985): M^2 of *K. piriyai* (MFT-K176; 17.5 and MFT-K180; 21.6), M_2 of *K. piriyai* (MFT-K177; 19.4 and MFT-K181; 21.4), as in *K. chiangmuanensis* (17.52; CHAIMANEE et al. 2003). The large-bodied *K. magnus* n. sp. (MFT-K178) M_2 displays the thickest enamel (23.9) and falls in the range of *G. blacki* (18.99–25.10; OLEJNICZAK et al. 2008). The holotype of *K. piriyai* (TF 6223; 15.65, range = 13.7–17.6; CHAIMANEE et al. 2004) has "intermediate thick" enamel. However, the enamel thickness of *K. piriyai*, *Sivapithecu*s and *Lufengpithecu*s fall within the variation attributed to extant *P. pygmaeus* (15.49, range = 8.60–22.50; OLEJNICZAK et al. 2008).

Relative dentine horn height

OLEJNICZAK et al. (2008) have established that among hominoids, pongids have relatively short dentine horns compared to African apes. The relative dentine horn height (RDHH) of *Khoratpithecus* specimens were compared with *S. sivalensis*, *G. blacki* and *Pongo pygmaeus* (Table 7). It appears that *Sivapithecus* upper molars have similar RDHH as *K. piriyai* (MFT-K176 and MFT-K180). Values of both taxa are higher than those of *Pongo* and *Gigantopithecus* but lower than those of *Pan* and *Gorilla* (OLEJNICZAK et al. 2008). Concerning the lower molars, the values of *K. piriyai* (MFT-K177 and MFT-K181) are similar to those of *Pongo* and *Gigantopithecus* but lower than to those of the holotypes of *K. piriyai* (TF 6223) and *K. chiangmuanensis*. More surprising is the very low value observed on the M_2 of the new species, *K. magnus* (MFT-K178) which might result from the difficulty to distinguish enamel from dentine on the micro-CT scan images of that specimen.

Body weight

Most Khorat specimens attributed to *K. piriyai* belong to large-bodied hominoids with an estimated body weight of 40–55 Kg (Table 8) based on cheek teeth (premolars and molars) occlusal area, according to the regressions proposed by GINGERICH et al. (1982). The body weight of MFT-K177 is 55.4 kg (range 38.7–63.3 kg), MFT-K181 is 54.2 (range 37.8–55.2 kg), MFT-K176 is 51.5 kg (range 42.6–68.0 kg) and MFT-K180 is 40.7 kg (range 36.1–48.7 kg). These body weight estimates are similar to those obtained for *K. piriyai* (TF 6223) (51 kg; range 34.6–54.0 kg). We assume therefore that these specimens might belong to male individuals because they show similar values to the males of *K. chiangmuanensis* (range 39.9–60.5 kg), which are significantly larger than females (range 23.5–29.2 kg). The large-bodied hominoid, *K. magnus* n. sp. (MFT-K178) has an estimated body weight of 73.7–82.0 kg, which is similar to that of *S. parvada* (BSPG 1939X4) (75.1 kg, range 52.1–98.3 kg).

Diet

The relationship between mandibular morphology and dietary categories is poorly understood (ROSS et al. 2012), but the deep and robust mandibular corpus deepening posteriorly in some individuals and the strongly buttressed symphysis suggest that the lower jaws of *Khoratpithecus* were adapted to resist high bone strains during mastication (HYLANDER et al. 1998; RAVOSA 2000; ROSS et al. 2012). The deep mandibular corpora are found in extant anthropoids categorized as folivores, seed predators, or hard-object feeders (RAVOSA 1996; DAEGLING & MCGRAW 2001; TAYLOR 2006; TAYLOR et al. 2008). The thick-enameled and high crowned molars, along with the tendency for heavy wear on the cheek teeth, point to dental adaptations for an abrasive diet (KONO et al. 2014). These characters, with the molariform premolars, relatively large molars, and long roots, suggest that *Khoratpithecus* was engaged in heavy mastication for processing hard and/or fibrous food (KUPCZIK & DEAN 2008). Two detailed studies have been previously devoted to the diet of *Khoratpithecus* species. The first was based on evidence from dental topographic and microwear texture analyses (MERCERON et al. 2006) and indicated that the teeth of *K. piriyai* and *K. chiangmuanensis* were better adapted to a frugivorous diet rather than to a folivorous one. But, in contrast to *K chiangmuanensi*s, food items consumed by *K. piriyai* required important masticatory movements. Results from microwear analyses indicate that *Khoratpithecus* consumed items similar to those consumed by extant hominoids in term of hardness and that it preferred soft fruits to hard fruits or seeds. A quantitative comparative analysis of the root morphology of *K. piriyai* (TF 6223; HAMON et al. 2012) concluded that its diet was mainly dominated by fruits (>50%), associated with animal matter (1–25%), leaves and vertebrates, seeds being excluded. These results are based on few specimens and the new set of fossil hominoids described here should allow a better understanding of the diet of *Khoratpithecus* and provide a better comparison with the diet of *Indopithecus* (PATNIAK et al. 2014). *Indopithecus* microwear and enamel stable isotope studies by PATNAIK et al. (2014)

concluded that it lived in a forested environment, a C3-dominated environment like that in which *Khoratpithecus* dwelt (JAEGER et al. 2011) and its main food might have been low-lying fruits, but also seeds, nuts, bark or even roots.

Phylogenetic affinities

We have recognized two distinct species among the new remains of *Khoratpithecus*, *K. piriyai* and *K. magnus* n. sp. These two species differ by their body size (Table 8), tooth sizes (text-figs. 10A, 10B) and proportions (Table 2, 4), enamel thickness (Table 6), mandibular dimension and morphology, and symphyseal breadth (Table 3). *Khoratpithecus piriyai* and *K. magnus* n. sp. lived in sympatry, a situation similar to that of the late Miocene of Siwaliks, where *S. indicus*, coexisted with a larger species, *I. giganteus* (PILBEAM et al. 1977; PILLANS et al. 2005). *Indopithecus* is considered a close relative of *Sivapithecus*, (BEGUN, 2015), as *K. magnus* n. sp. and *K. piriyai* are. At the same period, a third very large ape was evolving in South China which gave rise to the Pleistocene *G. blacki* VON KOENIGSWALD 1935, but unfortunately its remains are documented only from the Pleistocene of China (ZHANG & HARRISON 2017), Vietnam (CIOCHON et al. 1996) and Thailand (BOCHERENS et al. 2017). The late Miocene climatic and vegetational changes in South Asia are well documented in Siwaliks beds (BARRY et al. 2002). They might represent the cause of the homoplastic evolution of several distinct large-bodied hominoids with reduced incisor area, very massive and short jaws, and robust teeth with thick enamel, which were adapted to hard food.

Most hominoid taxa are currently recognized as sexually dimorphic (BROWN 1997). A pending problem concerns the sexual dimorphism within *Khoratpithecus* remains from the Khorat sand pit. Among the isolated teeth of *K. chiangmuanensis*, two different size clusters clearly appear to correspond to a normal sexual dimorphism (CHAIMANEE et al. 2003). However, the situation is much more obscure concerning the *Khoratpithecus* remains from

the Khorat sand pits. All individuals show nearly similar canine alveolar sizes. Therefore, this situation might result from the absence of female remains among the seven individuals documented. An alternative view would be to consider MFT-K178 as a male of *K. piriyai*, and all other individuals as females. However, as already mentioned, MFT-K178 has canine roots of similar size to those of *K. piriyai* but it also displays striking anatomical differences with the other specimens from the same area.

These new *Khoratpithecus* remains provide new information on the variability of the morphological characters among this genus. Some characters appear to be stable, like the lack of anterior digastric muscle scars, the low inclination of the symphysis (40° to 48°) relative to the alveolar plane, the premolar and molar dimensions, the cusp organization on the occlusal surfaces, the coarsely wrinkled enamel, the lack of cingula and cingulids, and the high robusticity index of the mandibular corpus, whereas other characters display some variation. The latter include the enamel thickness (Table 6), the relative dentine horn height (Table 7), the development of P_3 metaconid and the intercanine breadth. *Khoratpithecus piriyai* (TF 6223 holotype) displays a very large intercanine breadth and therefore its tooth rows have a characteristic bi-concave shape, with a maximal distance located at P_3 and M_3 levels. To the contrary, MFT-K177 has a reduced intercanine breadth, and therefore its tooth rows are divergent. On average, this last condition is more frequent, being documented in three individuals out of four, suggesting that *K. piriyai* had rather divergent teeth rows and smaller intercanine breadth than the holotype. This character corresponds to the primitive condition. It is also present in *Ankarapithecus* (ALGAPUT 1996 and *Sivapithecus* (PILBEAM et al. 1980). The relative dentine horn heights are similar to those of *S. sivalensis* for the upper molars and more similar to those of extant *Pongo* and *Gigantopithecus* for the lower molars in the specimens attributed to *K. piriyai* (Table 7). The symphyseal section also displays some

variability. The superior transverse torus is always thicker than the inferior transverse torus, which never developed into a simian shelf.

The morphological variation observed among the new specimens of *K. piriyai* indicates a slightly different image than was suggested by the holotype jaw, which displays close resemblance to *Pongo*, especially because of its wide anterior part of mandible, large intercanine breadth and procumbent incisors. The new individuals correspond rather to a hominoid with divergent tooth rows and narrow intercanine breadth. Enamel can reach high thickness values, dentine horns are short, as in other pongines, tooth wear is nearly horizontal, and the mandibular corpus is robust. Most of these characters are shared with *Indopithecus* and *Gigantopithecus* and have been interpreted as an adaptation to an abrasive diet. Nevertheless, some implications for the evolution of *Pongo* made by TAYLOR (2006) deserve moderation. According to TAYLOR (2006), most metric characters of the lower jaws of *K. piriyai* enter within the variation observed in extant *Pongo* for a similar jaw size to the exception of symphyseal inclination and M_3 corpus width. However, the high robusticity index observed at M_3 level cannot be related any more to the large buccolingual width of M_3 as mentioned by TAYLOR (2006) because two other jaws of *K. piriyai* (MFT-K177 and MFT-K181) display narrower M_3 associated with thicker corpus breadth. In any case, *Khoratpithecus* phylogenetic affinities remain close to *Pongo*, representing the closest sister group of that extant ape, excluding *Sivapithecus* and *Ankarapithecus* from this position. All *Khoratpithecus* specimens that preserve the ventral part of the symphysis lack the anterior digastric muscle scars indicating that this character, only shared with the extant *Pongo*, represents a constant characteristic of that genus. Symphyseal inclination and section are also indicative of *Pongo* affinities. The main differences concerning the symphysis are the lesser inclination in *Khoratpithecus* (JAEGER et al. 2011) and the extended simian shelf of the inferior transverse torus developed in *Pongo*, *Khoratpithecus* displaying a more primitive

structure of its inferior transverse torus. The occlusal surface of the lower premolars and molars also shares several characters, including the lack of cingula and cingulids, the coarsely wrinkled enamel in *Khoratpithecus* (finer wrinkled enamel in *Pongo*), the P_3 structure. However, *Pongo* differs by its larger intercanine breadth, wider incisive area, more procumbent incisors, larger canines, more extended P_4 talonids and more vertical buccal premolar and molar crown walls. As previously mentioned by CHAIMANEE et al. (2019), the upper maxilla also displays several characters that confirm close phylogenetic relationships between *Khoratpithecus* and *Pongo* while the minor differences in nasoalveolar clivus structure have been interpreted as corresponding to a more primitive character state when compared to extant *Pongo* (CHAIMANEE et al. 2019). However, some characters are also different, like the slanted buccal wall of the upper molars of *Khoratpithecus* and their smaller length/width ratio. These new data confirm the phylogenetic position of *Khoratpithecus* as the closest sister group of extant *Pongo*.

Conclusions

New specimens of Khorat hominoids described here greatly expand our knowledge of the genus *Khoratpithecus* and confirm its pongine affinities. They also illustrate its high morphological variability. Some diagnostic characters display no variation, such as the lack of anterior digastric muscle scars, the low symphyseal inclination angle and section outline, the dental morphology and the organization of the roots of cheek teeth (EMONET et al. 2012). Most of these characters are shared with *Pongo*. To the contrary, the corpus anatomy such as the intercanine breadth display large variation, which can modify the tooth row shape of some individuals. The robustness of the mandible and the enamel thickness of their molars are also variable. Among these new remains, a lower jaw fragment can be distinguished from the others by several morphological characters and is described as a new species of a larger sized

Khoratpithecus, *K. magnus* n. sp. Therefore, two sympatric hominoid species, one of medium size, another of large size, shared the same environment, a situation also known from the late Miocene Siwalik beds. This additional material does not modify the previous conclusions concerning the phylogenetic position of *Khoratpithecus,* but it confirms that *Khoratpithecus* is the closest sister group of *Pongo*. The dental topographic and the microwear texture analyses of the molar occlusal surfaces of these new remains will probably refine our knowledge concerning the diet of *Khoratpithecus*. Former data obtained on previous fossils *Khoratpithecus* indicated a fruit dominated diet, but new analysis might allow to determine the nature of the abrasive food associated to the heavy tooth wear and to the very strong robustness of some mandibles. Postcranial remains, which are still undocumented, should allow to document its locomotion and to clarify its phylogenetic relationships with *Pongo*.

Acknowledgements

This work has been supported by the CNRS-UMR 7262, the University of Poitiers and Department of Mineral Resources. We are grateful to K. Christopher Beard (University of Kansas), Louis de Bonis, Stéphane Ducrocq and Olivier Chavasseau (PALEVOPRIM) for valuable comments, discussion and providing comparative materials and documents. We thank Arnaud Mazurier and Jérôme Surault (PALEVOPRIM) for the CT-scan sections and photos, and Sabine Riffaut (PALEVOPRIM) for the figures. Daniela C. Kalthoff (Editor), Dr. Friedemann Schrenk and an anonymous reviewer helped to improve the manuscript with their helpful comments and suggestions.

References

ALPAGUT, B., ANDREWS, P., FORTELIUS, M., KAPPELMAN, J., TEMIZSOY, I., CELEBI, H., & LINDSAY, W. (1996). A new specimen of *Ankarapithecus meteai* from the Sinap Formation of central Anatolia. *Nature*, *382*, 349–351. https://doi.org/10.1038/382349a0

BARRY, J. C., MORGAN, M. L. E., FLYNN, L. J., PILBEAM, D., BEHRENSMEYER, A. K., RAZA, S. M., KHAN, I. A., BADGLEY, C., HICKS, J. & KELLEY, J. (2002). Faunal and environmental change in the late Miocene Siwaliks of northern Pakistan. *Paleobiology*, *28*, 1–71. https://doi.org/10.1666/0094-8373(2002)28[1:FAECIT]2.0.CO;2

BEGUN, D. R. (2015). Fossil Record of Miocene Hominoids. In W. HENKE, & I. E. TATTERSALL (Eds.), *Handbook of Palaeoanthropology Vol 2: Primate Evolution and Human Origins* (pp. 1261–1332). Berlin: Springer.

BEGUN, D. R., & GÜLEÇ, E. (1998) Restoration of the Type and Palate of *Ankarapithecus meteai*: Taxonomic and phylogenetic implications. *American Journal of Physical Anthropology*, *105*, 279–314. https://doi.org/10.1002/(SICI)1096-8644(199803)105:3<279::AID-AJPA2>3.0.CO;2-N

BHANDARI, A., KAY, R. F., WILLIAMS, B., TIWARI, B. N., BAJPAI, S., & HIERONYMUS, T. (2018). First record of the Miocene hominoid *Sivapithecus* from Kutch, Gujarat state, western India. *PLoS ONE 13*, e0206314. https://doi.org/10.1371/journal.pone.0206314

BOCHERENS, H., SCHRENK, F., CHAIMANEE, Y., KULLMER, O., MÖRIKE, D., PUSHKINA, D., & JAEGER, J.-J. (2017). Flexibility of diet and habitat in Pleistocene South Asian mammals: Implications for the fate of the giant fossil ape *Gigantopithecus*. *Quaternary International*, *434*, 148–155. http://dx.doi.org/10.1016/j.quaint.2015.11.059

BROWN, B. (1989). *The mandibles of Sivapithecus*. PhD thesis, Kent State University, Kent, Ohio.

BROWN, B. (1997). Miocene hominoid mandibles: Functional and phylogenetic perspectives. In D. R. BEGUN, C. V. WARD, & M. D. ROSE (Eds.), *Function, Phylogeny, and Fossils: Miocene Hominoid Evolution and Adaptations* (pp. 153–171). New York: Plenum Press.

CHAIMANEE, Y., JOLLY, D., BENAMMI, M., TAFFOREAU, P., DUZER, D., MOUSSA, I., & JAEGER, J.-J. (2003). A middle Miocene hominoid from Thailand and orangutan origins. *Nature*, *422*, 61–65. http://doi.org/10.1038/nature01449

CHAIMANEE, Y., LAZZARI, V., CHAIVANICH, K., & JAEGER, J.-J. (2019). First maxilla of a late Miocene hominid from Thailand and the evolution of pongine derived characters. *Journal of Human Evolution*, *134*, 102636. https://doi.org/10.1016/j.jhevol.2019.06.007

CHAIMANEE, Y., SUTEETHORN, V., JINTASAKUL, P., VIDTHAYANON, C., MARANDAT, B., & JAEGER, J.-J. (2004). A new orang-utan relative from the Late Miocene of Thailand. *Nature*, *427*, 439–441. http://doi.org/10.1038/nature02245

CHAIMANEE, Y., YAMEE, C., TIAN, P., KHAOWISET, K., MARANDAT, B., TAFFOREAU, P., NEMOZ, C., & JAEGER, J.-J. (2006). *Khoratpithecus piriyai*, a Late Miocene hominoid of Thailand. *American Journal of Physical Anthropology*, *131*, 311–323. http://doi.org/10.1002/ajpa.20437

CIOCHON, R., LONG, V. T., LARICK, R., GONZÁLEZ, L., GRÜN, R., VOS, J. D., YONGE, C., TAYLOR, L., YOSHIDA, H., & REAGAN, M. (1996). Dated co-occurrence of *Homo erectus* and *Gigantopithecus* from Tham Khuyen Cave, Vietnam. *Proceedings of the National Academy of Sciences*, *93*, 3016–3020. https://doi.org/10.1073/pnas.93.7.3016

COSTER, P., BENAMMI, M., CHAIMANEE, Y., YAMEE, C., CHAVASSEAU, O., EMONET, E.-G., & JAEGER, J.-J. (2010). A complete magnetic-polarity stratigraphy of the Miocene continental deposits of Mae Moh Basin, northern Thailand, and a reassessment of the

age of hominoid-bearing localities in northern Thailand. *Geological Society of America Bulletin*, *122*, 1180–1191. https://doi.org/10.1130/B26568.1

DAEGLING, D. J., & MCGRAW, W. S. (2001). Feeding, diet, and jaw form in West African *Colobus* and *Procolobus*. *International Journal of Primatology*, *22*, 1033–1055. https://doi.org/10.1023/A:1012021823076

DENG, T., HANTA, R., & JINTASAKUL, P. (2013). A new species of *Aceratherium* (Rhinocerotidae, Perissodactyla) from the late Miocene of Nakhon Ratchasima, northeastern Thailand. *Journal of Vertebrate Paleontology*, *33*, 977–985. https://doi.org/10.1080/02724634.2013.748058

DUANGKRAYOM, J., WANG, S., DENG, T. & JINTASAKUL, P. (2017). The first Neogene record of *Zygolophodon* (Mammalia, Proboscidea) in Thailand: implications for the mammutid evolution and dispersal in Southeast Asia. *Journal of Paleontology*, *91*, 179–193. https://doi.org/10.1017/jpa.2016.143

EMONET, E.-H., TAFFOREAU, P., CHAIMANEE, Y., GUY, F., de BONIS, L., KOUFOS, G. & JAEGER, J.-J. (2012). Three-dimensional analysis of mandibular dental root morphology in hominoids. *Journal of Human Evolution*, *62*, 146–154. https://doi.org/10.1016/j.jhevol.2011.11.011

FUSS, J., SPASSOV, N., BEGUN, D. R., & BÖHME, M. (2017). Potential hominin affinities of *Graecopithecus* from the Late Miocene of Europe. *PLoS ONE 12*, e0177127. https://doi.org/10.1371/journal.pone.0177127

GINGERICH, P. D., SMITH, B. H., & ROSENBERG, K. (1982). Allometric scaling in the dentition of primates and prediction of body weight from tooth size in fossils. *American Journal of Physical Anthropology*, *58*, 81–100. https://doi.org/10.1002/ajpa.1330580110

HAMON, N., EMONET, E.-G., CHAIMANEE, Y., GUY, F., TAFFOREAU, P., & JAEGER, J.-J. (2012). Analysis of Dental Root Apical Morphology: A new method for Dietary

Reconstructions in Primates. *The Anatomical Record*, *295*, 1017–1026. https://doi.org/10.1002/ar.22482

HANDA, N., NISHIOKA, Y., DUANGKRAYOM, J., & JINTASAKUL, P. (2020). *Brachypotherium perimense* (Perissodactyla, Rhinocerotidae) from the Miocene of Nakhon Ratchasima, Northeastern Thailand, with comments on fossil records of *Brachypotherium*. *Historical Biology*, *33*, 1642-1660. https://doi.org/10.1080/08912963.2020.1723578

HANTA, R., RATANASTHIEN, B., KUNIMATSU, Y., SAEGUSA, H., NAKAYA, H., NAGAOKA, S., & JINTASAKUL, P. (2008). A new species of Bothriodontinae, *Merycopotamus thachangensis* (Cetartiodactyla, Anthracotheriidae) from the Late Miocene of Nakhon Ratchasima, northeastern Thailand. *Journal of Vertebrate Paleontology*, *28*, 1182–1188. https://doi.org/10.1671/0272-4634-28.4.1182

HYLANDER, W. L., RAVOSA, M. J., ROSS, C. F., & JOHNSON, K. R. (1998). Mandibular corpus strain in primates: further evidence for a functional link between symphyseal fusion and jaw-adductor muscle force. *American Journal of Physical Anthropology*, *107*, 257–271. https://doi.org/10.1002/(SICI)1096-8644(199811)107:3<257::AID-AJPA3>3.0.CO;2-6

JAEGER, J.-J., AUNG NAING SOE, CHAVASSEAU, O., COSTER, P., EMONET, E., GUY, F., LEBRUN, R., AYE MUANG, AUNG AUNG KHYAW, HLA SHWE, SOE TURA TUN, KYAW LINN OO, RUGBUMRUNG, M. BOCHERENS, H. BENAMMI, M., CHAIVANICH, K., TAFFOREAU, P. & CHAIMANEE, Y. (2011). First Hominoid from the Late Miocene of the Irrawaddy Formation (Myanmar). *PLoS ONE*, *6,* e17065. https://doi.org/10.1371/journal.pone.0017065

KAPPELMAN, J., RICHMOND, B. G., SEIFFERT, E. R., MAGA, A. M., & RYAN, T. M. (2003). Hominoidea (Primates). In M. FORTELIUS, J. KAPPELMAN, S. SEN, & L. BERNOR (Eds.), *Geology and Paleontology of the Miocene Sinap Formation, Turkey* (pp. 90–124). New York: Columbia University Press.

KELLEY, J. (1988). A new large species of *Sivapithecus* from the Siwaliks of Pakistan. *Journal of Human Evolution*, *17*, 305–324. https://doi.org/10.1016/0047-2484(88)90073-5

KELLEY, J., & XU Q. (1991). Extreme sexual dimorphism in a Miocene hominoid. *Nature*, *352*, 151–153. https://doi.org/10.1038/352151a0

KOENIGSWALD, G. H. R. Von (1935). Eine fossile Säugetierfauna mit *Simia* aus Sudchina. *Proceeding of the Koninklijke Nederlandse Akademie van Wetenschappen*, *38*, 872–879.

KOENIGSWALD, G. H. R. VON (1951) Remarks on *Indopithecus*: a reply. *American Journal of Physical Anthropology*, *9*, 461–464. https://doi.org/10.1002/ajpa.1330090407

KONO, R. T., ZHANG, Y., JIN, C., TAKAI, M., & SUWA, G. (2014). A 3-dimensional assessment of molar enamel thickness and distribution pattern in *Gigantopithecus blacki*. *Quaternary International*, *354*, 46–51. https://doi.org/10.1016/j.quaint.2014.02.012

KUPCZIK, K., & DEAN, M. C. (2008). Comparative observations on the tooth root morphology of *Gigantopithecus blacki*. *Journal of Human Evolution*, *54*, 196–204. https://doi.org/10.1016/j.jhevol.2007.09.013

LI, S., DENG, C., DONG, W., SUN, L., LIU, S., QIN, H., YIN, J., JI, X., & ZHU, R. (2015). Magnetostratigraphy of the Xiaolongtan Formation bearing *Lufengpithecus keiyuanensis* in Yunnan, southwestern China: Constraint on the initiation time of the southern segment of the Xianshuihe–Xiaojiang fault. *Tectonophysics*, *655*, 213–226. https://doi.org/10.1016/j.tecto.2015.06.002

LIHOREAU, F., BARRY, J., BLONDEL, C., CHAIMANEE, Y., JAEGER, J.-J., & BRUNET, M. (2007). Anatomical revision of the genus *Merycopotamus* (Artiodactyla; Anthracotheriidae): its significance for Late Miocene mammal dispersal in Asia. *Palaeontology*, *50*, 503–524. https://doi.org/10.1111/j.1475-4983.2006.00643.x

MAHONEY, P., SMITH, T. M., SCHWARTZ, G. T., DEAN, C., & KELLEY, J. (2007). Molar crown formation in the Late Miocene Asian hominoids, *Sivapithecus parvada* and *Sivapithecus indicus*. *Journal of Human Evolution*, *53*, 61–68. https://doi.org/10.1016/j.jhevol.2007.01.007

MARTIN, L. B. (1985). Significance of enamel thickness in hominid evolution. *Nature*, *314*, 260-263. https://doi.org/10.1038/314260a0

MERCERON, G., TAYLOR, S., SCOTT, R., CHAIMANEE, Y., & JAEGER, J.-J. (2006). Dietary characterization of the hominoid *Khoratpithecus* (Miocene of Thailand): evidence from dental topographic and microwear texture analyses. *Naturwissenschaften*, *93*, 329–333. https://doi.org/10.1007/s00114-006-0107-0

NISHIOKA, Y., HANTA, R., & JINTASAKUL, P. (2014). Note on giraffe remains from the Miocene of continental Southeast Asia. *Journal of Science and Technology MSU*, *33*, 365-377.

NISHIOKA, Y., VIDTHAYANON, C., HANTA, R., DUANGKRAYOM, J., & JINTASAKUL, P. (2020). Neogene Bovidae from Tha Chang sand pits, Nakhon Ratchasima, Northeastern Thailand. *Thailand Natural History Museum Journal*, *14*, 59–72.

OLEJNICZAK, A. J., SMITH, T. M., WANG, W., POTTS, R., CIOCHON, R., KULLMER, O., SCHRENK, F., & HUBLIN, J.-J. (2008). Molar enamel thickness and dentine horn height in *Gigantopithecus blacki*. *American Journal of Physical Anthropology, 135*, 85–91. https://doi.org/10.1002/ajpa.20711

OZANSOY, F. (1965). Étude des gisements continentaux et des mammifères du Cénozoique de Turquie. *Mémoires de la Société Géologique de France*, 44, 1–92.

PATNAIK, R., CERLING, T. E., UNO, K. T., & FLEAGLE, J. G. (2014). Diet and habitat of Siwalik primates *Indopithecus*, *Sivaladapis* and *Theropithecus*. *Annales Zoologici Finnici*, *51*, 123–142. https://doi.org/10.5735/086.051.0214

PILBEAM, D., MEYER, G. E., BADGLEY, C., ROSE, M. D., PICKFORD, M. H. L., BEHERENSMEYER, A. K., & SHAH, S. M. I. (1977) New hominoid primates from the Siwaliks of Pakistan and their bearing on hominoid evolution. *Nature*, *270*, 689–695. https://doi.org/10.1038/270689a0

PILBEAM, D., ROSE, M. D., BADGLEY, C., & LIPSCHUTZ, B. (1980). Miocene Hominoids from Pakistan. *Postilla*, *181*, 1–94.

PILGRIM, G. E. (1915). New Siwaliks primates and their bearing on the question of the evolution of man and the Anthropoidea. *Records of the Geological Survey of India*, *45*, 1–74.

PILLANS, B., WILLIAMS, M., CAMERON, D., PATNAIK, R., HOGARTH, J., SAHNI, A., SHARMA, J. C., WILLIAMS, F., & BERNOR, R. (2005). Revised correlation of the Haritalyangar magnetostratigraphy, Indian Siwaliks: implications for the age of the Miocene hominids *Indopithecus* and *Sivapithecus*, with a note on a new hominid tooth. *Journal of Human Evolution*, *48*, 507–515. https://doi.org/10.1016/j.jhevol.2004.12.003

PREUSS, T. M. (1982). The face of *Sivapithecus indicus*: description of a new, relatively complete specimen from the Siwaliks of Pakistan. *Folia Primatologica, 38,* 141–157. https://doi.org/10.1159/000156053

RAVOSA, M. J. (1996). Jaw morphology and function in living and fossil Old World monkeys. *International Journal of Primatology*, *17*, 909–932. https://doi.org/10.1007/BF02735294

RAVOSA, M. J. (2000). Size and scaling in the mandible of living and extinct apes. *Folia Primatologica*, *71*, 305–322. https://doi.org/10.1159/000021754

ROSS, C. F., IRITATE-DIAZ, J., & NUNN, C. L. (2012). Innovative approaches to the relationship between diet and mandibular morphology in primates. *International Journal of Primatology*, *33*, 632–660. https://doi.org/10.1007/s10764-012-9599-y

SAEGUSA, H., THASOD, Y., & RATANASTHIEN, B. (2005). Notes on Asian stegodontids. *Quaternary International*, *126-128*, 31–48. https://doi.org/10.1016/j.quaint.2004.04.013

SCHINDELIN, J., ARGANDA-CARRERAS, I., FRISE, E., KAYNIG, V., LONGAIR, M., PIETZSCH, T., PREIBISCH, S., RUEDEN, C., SAALFELD, S., SCHMID, B., TINEVEZ, J.-Y., WHITE, D. J., HARTENSTEIN, V., ELICEIRI, K., TOMANCAK, P., & CARDONA, A. (2012). Fiji: an open-source platform for biological-image analysis. *Nature Methods, 9*, 676–682. https://doi.org/10.1038/nmeth.2019

SEPULCHRE, P., JOLLY, D., DUCROCQ, S., CHAIMANEE, Y., JAEGER, J.-J., & RAILLARD, A. (2010). Mid-Tertiary paleoenvironments in Thailand: pollen evidences. *Climates of the Past*, *6*, 461–473. https://doi.org/10.5194/cp-6-461-2010

SIMONS, E. L., & CHOPRA, S. R. K. (1969). *Gigantopithecus* (Pongidae, Hominoidea) a new species from North India. *Postilla*, *138*, 1–18.

SMITH, T. M., MARTIN, L. B., & LEAKEY, M. G. (2003). Enamel thickness, microstructure and development in *Afropithecus turkanensis*. *Journal of Human Evolution*, *44*, 283–306. https://doi.org/10.1016/S0047-2484(03)00006-X

TAKAI, M., KHIN NYO, KONO, R. T., THAUNG HTIKE, KUSUHASHI, N., & ZIN MUANG MUANG THEIN (2021). New hominoid mandible from the early Late Miocene Irrawaddy Formation in Tebingan area, central Myanmar. *Anthropological Science*, *129*, 87–98. https://doi.org/10.1537/ase.2012131

TAYLOR, A. B. (2006). Feeding behavior, diet, and the functional consequences of jaw form in orangutans, with implications for the evolution of *Pongo*. *Journal of Human Evolution*, *50*, 377–393. https://doi.org/10.1016/j.jhevol.2005.10.006

TAYLOR, A. B., VOGEL, E. R., & DOMINY, N. J. (2008). Food material properties and mandibular load resistance abilities in large-bodied hominoids. *Journal of Human Evolution*, *55*, 604–616. https://doi.org/10.1016/j.jhevol.2008.04.001

THASOD, Y., JINTASAKUL, P., & RATANASTHIEN, B. (2012). Proboscidean fossil from the Tha Chang sand pits, Nakhon Ratchasima Province, Thailand. *Journal of Science and Technology MSU*, *31*, 33–44.

WARD, S. (1997). The taxonomy and phylogenetic relationships of *Sivapithecus* revisited. In D. R. BEGUN, C. V. WARD, & M. D. ROSE (Eds.), *Function, Phylogeny, and Fossils: Miocene Hominoid Evolution and Adaptations* (pp. 269–290). New York: Plenum Press.

WOO, R. (1957). *Dryopithecus* teeth from Keiyuan, Yunnan Province. *Vertebrata PalAsiatica*, *1*, 25–32.

XU, Q., LU, Q., PAN, Y., ZHENG, X., & ZHENG, L. (1978). Fossil mandible of the Lufeng *Ramapithecus*. *Kexue Tongbao*, *9*, 554–556.

XU, Q. H., & LU, Q. W. (2008). *Lufengpithecus lufengensis-an early member of Hominidae*. Beijing: Science Press.

YUE, L. P., & ZHANG, Y. X. (2006). Paleomagnetic dating of *Lufengpithecus hudienensis* localities (in Chinese). In G. QI, & W DONG (Eds.), *Lufengpithecus hudienensis Site* (pp. 245–255). Beijing: Science Press.

ZHANG, L.-Z., DU, B.-P., GAO, F., & ZHAO, L.-X. (2021). A micro-CT based study of molar enamel thickness and its distribution pattern in Late Miocene *Lufengpithecus lufengensis* from Yunnan in Southwestern China. *Historical Biology*, *33*, 2236–2246. https://doi.org/10.1080/08912963.2020.1782395

ZHANG, X., LIN, Y., JIANG, C., & XIAO, L. (1987). A new species of *Ramapithecus* from Yuanmou, Yunnan. *Journal Yunnan University (Social Sciences) 3*, 54–56.

ZHANG, Y., & HARRISON, T. (2017). *Gigantopithecus blacki*: a giant ape from the Pleistocene of Asia revisited. *American Journal of Physical Anthropology*, *162*, 153–177. https://doi.org/10.1002/ajpa.23150

ZHENG, L. (2006). *Lufengpithecus hudienensis* fossils (in Chinese). In G. QI & W. DONG (Eds.) *Lufengpithecus hudienensis Site* (pp. 40–74). Beijing: Science Press.

Table 1 List of hominoid mandibles and maxillae recovered from Khorat sand pits, Thailand.

Specimen no.	Description	References
MFT-K177 (*Khoratpithecus piriyai*)	Mandible fragment with well-preserved left P_4-M_3 and right P_3-M_3, alveolar fragments of I_1, I_2, and C and root of left P_3.	This study
MFT-K181 (*K. piriyai*)	Left mandible fragment with well-preserved P_3-M_3 and alveoli of I_1, I_2 and C.	This study
MFT-K180 (*K. piriyai*)	Left maxillary fragment with well-preserved P^3-M^3 and fragment of root alveoli of left I^2 and C.	This study
MFT-K178 (*K. magnus* n. sp.)	Mandible fragment with well-preserved left P_4-M_2, alveolar fragments of C and P_3 and root of right P_4.	This study
MFT-K179 (*Khoratpithecus* sp.)	Mandible fragment, missing tooth crowns, only roots of left C-M_1 and right C-M_2 being preserved with alveolar fragments of I_1 and I_2.	This study
TF 6223 (*K. piriyai*)	Mandible fragment with well-preserved left P_3-M_3 and right C-M_3, the root alveoli of I_1 and root fragments of I_2 and left C. (Holotype)	CHAIMANEE et al. (2004)
MFT-K176 (*K. piriyai*)	Maxilla fragment with well-preserved left I^2-M^3 and right P^3-M^3, the alveoli of the left and right I^1 and right C, and root of right I^2.	CHAIMANEE et al. (2019)

Table 2. Measurements of lower dentitions (in mm) of *Khoratpithecus piriyai* (MFT-K177 and MFT-K181) and of *K. magnus* n. sp. (MFT-K178) compared with *K. piriyai* (TF 6223 holotype; CHIAMANEE et al. 2004), *K. ayeyarwadyensis* (MFI-K171 holotype; JAEGER et al. 2011) and MZKB-K-001 (TAKAI et al. 2021); upper dentition of *K. piriyai* (MFT-K180) compared with *K. piriyai* (MFT-K176; CHAIMANEE et al. 2019). MD (Mesiodistal length), BL (Buccolingual width), trig/tal (trigonid/talonid), Left (L), Right (R), * estimated value.

	K. piriyai						*K. magnus* n. sp.		*K. ayeyarwadyensis*		MZKB-K-001	
	MFT-K177		MFT-K181		TF 6223		MFT-K178		MFI-K171			
	MD	BL (trig/tal)	MD	BL (trig/tal)	MD	BL (trig/tal)	MD	BL (trig/tal)	MD	BL (trig/tal)	MD	BL (trig/tal)
P_3L	-	-	14.29	9.09	13.79	8.51	-	-	13.5	9.68	-	-
P_3R	11.60	11.69	-	-	14.57	8.53	-	-	-	-	-	-
P_4L	10.30	11.31	9.61	9.63	9.61	10.63/10.53	11.76	11.89	8.19	9.92	-	-
P_4R	10.23	11.45	-	-	9.24	10.65/10.23	-	-	-	-	-	-
M_1L	12.27	11.47*/11.47	12.54	11.38/11.04	12.88	10.53/11.30	14.24	12.17/11.84	12.29	11.05/10.33	-	-
M_1R	13.04	11.58*/12.13	-	-	12.38	10.69/11.34	-	-	-	-	-	-
M_2L	13.71	13.20/12.91	15.12	13.58/12.76	13.76	12.86/12.88	18.24	14.60/13.99	13.92	12.75/11.46	13.90	12.30*/11.30
M_2R	13.64	13.55/12.97	-	-	13.77	12.68/12.72	-	-	-	-	-	-
M_3L	14.89	12.37/11.76	15.62	13.77/11.17	17.73	14.68/13.16	-	-	14.20*	11.93/9.25*	14.65	13.00*/12.20
M_3R	15.53	13.37/12.22	-	-	17.63	14.71/13.12	-		-	-	-	-

	K. piriyai			
	MFT-K180		MFT-K176	
	MD	BL (mesial/ distal)	MD	BL
P^3L	8.53	11.62	8.13	14.00
P^3R	-	-	8.10	14.06
P^4L	7.61	11.76	8.28	13.38
P^4R	-	-	8.28	13.23
M^1L	11.36	12.83/12.86	11.59	15.53*
M^1R	-	-	11.43	15.55*
M^2L	11.49	14.95/13.93	12.83	16.32
M^2R	-	-	12.75	16.36
M^3L	12.66	15.59/12.93	12.59	14.32
M^3R	-	-	12.42	15.16
P^3-M^3 length	51.43		52.13	
P^3-P^4 length	15.72		15.96	
M^1-M^3 length	36.65		36.43	

Table 3. Mandibular dimensions (in mm) of *Khoratpithecus piriyai* (MFT-K177 and MFT-K181), *K. magnus* n. sp. (MFT-K178) and *Khoratpithecus* sp. (MFT-K179) compared with *K. piriyai* (TF 6223; CHAIMANEE et al. 2004, 2006), *K. ayeyarwadyensis* (MFI-K171; JAEGER et al. 2011), MZKB-K-001 (TAKAI et al. 2021) and *Indopithecus giganteus* (CYP 359/68; SIMONS & CHOPRA 1969). Left (L), Right (R), * estimated value.

		K. piriyai		*K. magnus*	*Khoratpithecus* sp.	*K. ayeryarwadyensis*	MZKB-K-001	*I. giganteus*
	MFT-K177	MFT-K181	TF 6223	MFT-178	MFT-179	MFI-K171		CYP 359/68
P_3-M_3 length	67.16 (R)	67.18	63.93	-	-	61.02*	-	77.80
P_3-P_4 length	22.48 (R)	22.07	21.10	-	-	19.23	-	24.36
M_1-M_3 length	44.0 (L)-43.73 (R)	44.06	42.97	-	-	41.15*	-	53.56
Intercanine breadth	18.71	18.30*	31.35	17.86*	15.47	-	-	13.60
Intercanine breadth /MD length M_2	1.37	-	2.27	0.98	-	-	-	0.73
Mental foramen								
Position under	P_3 mesial	P_3 middle	P_3 mesial	P_3 mesial	P_3/P_4	C/P_3	P_3	P_4
Distance from alveolar margin	16.10	24.60	24.20	28.71*	26.60*	22.80	-	26

Distance between left and right	29.36	-	39.00	29.70	27.80	-	-	45.60
Symphyseal								
Extension to	M_1 distal	M_1 distal	M_1 mesial	M_1 distal	M_1 distal	P_4/M_1	P_4/M_1	M_1 distal
Length	>47.50	>53.0	54.40	>50.0	>50.0	>34.81	-	-
Breadth at superior transverse torus	25.0	22.22	21.00	28.75	24.0	17.33	-	28.40
Breadth at inferior transverse torus	17.50	16.80	13.51	13.75	15.70	13.68	-	-
Inclination angle	40°	45°	42°	40°	43°	48°	-	64°

Table 4. Dental proportions)MD length/BL width × 100, in %**)** of lower and upper teeth of *Khoratpithecus piriyai* (MFT-K177, MFT-K181 and MFT-K180) and *K. magnus* n. sp. (MFT-K178) compared with other Asian hominoids. *K. piriyai* (TF 6223 data from CHAIMANEE et al. 2004; MFT-K176 data from CHAIMANEE et al. 2019), *K. ayeyarwadyensis* (MFI-K171; data from JAEGER et al. 2011), MZKB-K-001 (data from TAKAI et al. 2021), *Sivapithecus* (data from BEGUN & GÜLEÇ 1998), *S. parvada* (data from KELLEY 1988), *Indopithecus giganteus* (data from SIMONS & CHOPRA 1969), *Gigantopithecus blacki* (data from SIMONS & CHOPRA 1969) and *Pongo* (data from BEGUN & GÜLEÇ 1998). Mean, ranges and sample sizes in parentheses, * estimated value.

	K. piriyai			*K. magnus*	*K. ayeyarwadyensis*	MZKB-K-001	*Sivapithecus*	*S. parvada*	*I. giganteus*	*G. blacki*	*Pongo*
	MFT-K177	MFT-K181	TF 6223	MFT-K178	MFI-K171						
P_3	99	157	167	–	139	–	–	175	–	–	–
	–	–	162–171 (2)	–	–	–	–	173–176 (2)	–	–	–
P_4	90	100	90	99	83	–	86	92	–	–	94
	89–91 (2)	–	89–91 (2)	–	–	–	74–100 (21)	89–94 (2)	–	–	83–100 (13)
M_1	109	112	115	119	115	–	112	107	120	108	110
	107–110 (2)	–	118–112 (2)	–	–	–	106-128 (15)	96–104 (4)	–	102–117 (3)	103-123 (125)
M_2	104	115	108	128	115	118	116	104	119	107	107
	103–105 (2)		107–108 (2)	–	-	-	103-119 (19)	103–104 (2)	–	101–113 (3)	94-133 (110)

M_3	122	126	127	–	134*	116	–	104	121	–	–
	121–123 (2)	–	127–127 (2)	–	–	–	–	–	–	–	–

	K. piriyai		*Sivapithecus*	*S. parvada*	*Pongo*
	MFT-K180	MFT-K176			
P^3	73	58	74	70	77
	–	58–58 (2)	60–82 (9)	–	61–103 (58)
P^4	65	63	66	59	73
	–	62–63 (2)	56–77 (15)	56–62 (2)	64–81 (59)
M^1	88	75	90	82	92
	–	74–75 (2)	75–100 (27)	75–89 (4)	80–102 (60)
M^2	80	79	89	82	88
	–	78–79 (2)	80–99 (17)	–	78–98 (61)
M^3	89	85	–	77	–
	–	82–88 (2)	–	–	–

Table 5. Mandibular corpus dimensions (corpus height and breadth) and robusticity index (RI, corpus breadth/corpus height x 100) of *Khoratpithecus piriyai* (MFT-K177 and MFT-K181), *Khoratpithecus magnus* n. sp. (MFT-K178), *Khoratpithecus* sp. (MFT-K179) compared with *K. piriyai* (TF 6223 holotype; CHAIMANEE et al. 2004), *K. ayeyarwadyensis* (MFI-K171 holotype; JAEGER et al. 2011) and MZKB-K-001 (TAKAI et al. 2021).

	K. piriyai			*K. magnus* n. sp.	*Khoratpithecus* sp.	*K. ayeyarwadyensis*	MZKB-K-001
	MFT-K177	MFT-K181	TF 6223	MFT-K178	MFT-K179	MFI-K171	
Corpus height at P_4	35.64 (L)-35.31 (R)	45.93	38.88	41.80	36.97	33.14	39.88
Corpus breadth at P_4	25.18 (L)-24.97 (R)	21.16	21.23	>26.23	14.77	17.87	20.54
RI at P_4	71	46	55	-	40	54	52
Corpus height at M_1	36.73 (L)-39.09 (R)	45.98	40.61	-	37.34	33.04	39.34
Corpus breadth at M_1	29.85 (L)-31.97 (R)	23.84	19.84	>24.60	19.65	15.98	19.05
RI at M_1	82	52	49	-	53	48	48
Corpus height at M_2	42.48 (L)-40.72 (R)	46.40	37.67	-	-	31.86	37.54
Corpus breadth at M_2	28.23 (L)-30.13 (R)	28.15	28.43	-	-	18.67	18.28
RI at M_2	71	61	75	-	-	59	49
Corpus height at M_3	46.69 (L)-47.30 (R)	49.31	40.19	-	-	36.51	37.02
Corpus breadth at M_3	33.00 (L)-34.48 (R)	32.66	31.43	-	-	21.39	23.81
RI at M_3	72	66	78	-	-	59	64

Table 6. Two-dimensional dental tissue proportions and enamel thickness measurements (mean, minimum, and maximum) of *Khoratpithecus* compared to other Asian fossil and extant hominoids. N (number of specimens); EDJ: length of the enamel-dentine junction (mm); EC: enamel cap area (mm^2); AET: 2D AET: average enamel thickness (mm); CD: coronal dentine area (mm^2); 2D RET: relative enamel thickness (%). Enamel thickness categories by Martin (1985) based on mean 2D RET values: Thick (>17.49), Intermediate thick (14.65 – 17.49), Intermediate thin (11.31 – 14.64), Thin (<11.30).

Taxon	N	EDJ	EC	2D AET	CD	2D RET	References	Category
Khoratpithecus piriyai								
TF 6223	2	-	-	-	-	15.65 (13.7-17.6)	Chaimanee et al. (2006)	Intermediate thick
MFT-K177 (M_2)	1	21.1	29.8	1.41	53.1	19.4	This study	Thick
MFT-K181 (M_2)	1	19.1	29.2	1.53	50.9	21.4	This study	Thick
MFT-K176 (M^2)	2	21.7 (20.6-22.7)	27.9 (24.7-31.0)	1.29 (1.20-1.37)	54.2 (50.1-58.3)	17.5 (17.0-17.9)	This study	Thick
MFT-K180 (M^2)	1	19.6	28.7	1.46	45.9	21.6	This study	Thick
K. magnus n. sp. MFT-K178 (M_2)	1	21.65	38.79	1.79	56.30	23.90	This study	Thick
K. chiangmuanensis	2	-	-	-	-	17.52	Chaimanee et al. (2003)	Thick

						(17.23-17.80)		
Gigantopithecus blacki	7	32.59 (28.63-35.41)	79.76 (53.61-107.15)	2.42 (1.87-3.06)	122.50 (89.97-151.45)	21.77 (18.99-25.10)	Olejniczak et al. (2008)	Thick
Sivapithecus sivalensis	3	-	-	-	-	19.2 (16.3-20.9)	Smith et al. (2003)	Thick
S. parvada (M_1)	1	-	-	-	-	18.9	Mahoney et al. (2007)	Thick
S. indicus (M^1)	1	-	-	-	-	16.5	Mahoney et al. (2007)	Intermediate thick
Lufengpithecus lufengensis	68	18.22 (13.93-25.40)	19.72 (11.27-39.90)	1.08 (0.73-1.81)	37.49 (23.10-64.74)	17.95 (11.36-28.40)	Zhang et al. (2021)	Thick
L. hudienensis	1	-	-	-	-	14.10	Smith et al. (2003)	Intermediate thin
Pongo pygmaeus	41	21.34 (16.12-25.79)	23.42 (17.42-31.86)	1.10 (0.72-1.38)	50.93 (31.47-70.56)	15.49 (8.60-22.50)	Olejniczak et al. (2008)	Intermediate thick

Table 7. Relative dentine horn height of *Khoratpithecus* compared with other hominoids. Values in percentage, * (mean value; data from OLEJNICZAK et al. 2008).

Taxa	Tooth	Protocone	Paracone	Protoconid	Metaconid
Khoratpithecus piriyai					
TF 6223	LM_1	-	-	35.7	37.2
TF 6223	LM_2	-	-	32.3	41.1
MFT-K177	LM_2	-	-	21.7	26.3
MFT-K181	LM_2	-	-	28.6	26.3
MFT-K176	LM^2	28.0	35.4	-	-
MFT-K176	RM^2	30.3	36.2	-	-
MFT-K180	LM^2	30.0	36.2	-	-
K. magnus n. sp. (MFT-K178)	LM_2	-	-	15.2	12.2
K. chiangmuanensis (TF 6171-5)	LM_2	-	-	32.6	33.5
*Gigantopithecus blacki**		23.9	22.3	28.4	27.2
*Sivapithecus sivalensis**		32.1	35.8	-	-
*Pongo pygmaeus**		28.2	27.1	28.0	30.7
*Pan troglodytes**		34.7	37.3	-	-
*Gorilla gorilla**		40.4	38.2	-	-

Table 8. Estimated body weight (kg) measurements obtained from the teeth crown areas following GINGERICH et al. (1982).

Lower teeth of *Khoratpithecus piriyai* (MFT-K177 and MFT-K 181 data from Table 2) and TF 6223 (data from CHAIMANEE et al. 2004); *K. magnus* n. sp. (MFT-K178 data from Table 2); *K. ayeyarwadyensis* (MFI-K171 data from JAEGER et al. 2011), *K. chiangmuanensis* (data from CHAIMANEE et al. 2003) and *Sivapithecus parvada* (BSPG 1939X4 data from KELLEY 1988). Upper teeth of *K. piriyai* (MFT-K180 data from Table 2 and MFT-K176 data from CHAIMANEE et al. 2019), *K. chiangmuanensis* (data from CHAIMANEE et al. 2003) and *Khoratpithecus* sp. (MFI 89 data from JAEGER et al. 2011).

Teeth	*K. piriyai*			*K. magnus* n. sp.	*K. ayeyarwadyensis*	*K. chiangmuanensis*		*S. parvada*
	MFT-K177	MFT-K 181	TF 6223	MFT-K178	MFI-K171	male	female	BSPG 1939X4
P_3	39.77	37.75	34.58	-	38.03	-	-	52.07
P_4	63.27	45.25	49.91	81.98	37.51	60.48	29.23	98.28
M_1	59.42	55.22	54.00	73.91	49.93	-	-	68.54
M_2	45.35	51.77	44.06	73.73	41.62	40.92	23.46	59.70
M_3	38.71	40.06	52.70	-	29.60	39.90	-	52.74
∑cheekteeth	55.38	54.17	56.51	-	45.04	-	-	75.07

Teeth	*K. piriyai*		*K. chiangmuanensis*		*Khoratpithecus* sp.
	MFT-K180	MFT-K176	male	female	MFI 89
P^3	44.66	54.37	37.39	-	-
P^4	36.90	50.72	-	-	-
M^1	48.69	68.02	-	-	-
M^2	36.05	49.46	-	18.68	42.9
M^3	41.57	42.61	-	18.03	-
∑ cheekteeth	40.69	51.49	-	-	-

Figure captions

Text-fig. 1. Mandible of *Khoratpithecus piriyai* (MFT-K177). A: Occlusal view. B: Inferior view. C: Posterior view. D: Left lateral view. E: Anterior view. F: Right lateral view. (A-F) photographic image. Scale bar is 2 cm.

Text-fig. 2. Virtual reconstitute of the mandible of *Khoratpithecus piriyai* (MFT-K177) by using symmetric of the right jaw. A: occlusal view. B: Inferior view. C: Anterior view. Images are digital renderings of 3D virtual model generated from µCT scan data. Scale bar is 2 cm.

Text-fig. 3. *Khoratpithecus piriyai* (MFT-K177). A: Longitudinal slice through left ramus. B: Coronal-sections display positions of all slices (1-12). C: Midsagittal slice through symphysis. (A-C) Images are digital renderings of 3D virtual model generated from µCT scan data. Scale bar is 2 cm.

Text-fig. 4. Midsagittal slices through symphysis. A-C *Khoratpithecus piriyai*. A: MFT-K177 (mirror), B: MFT-K181 (mirror), C: TF 6223. D: *Khoratpithecus magnus* n. sp. (MFT-K178; mirror). E: *Khoratpithecus* sp. (MFT-K179). F: *Khoratpithecus ayeyarwadyensis* (MFI-K171; mirror). (A-E) Images are digital renderings of 3D virtual model generated from µCT scan data. Not to scale.

Text-fig. 5. Morphology of roots of *Khoratpithecus piriyai* (MFT-K177). A: Inferior view. B: Right buccal view. C: Right lingual view. Images are digital renderings of 3D virtual model generated from µCT scan data. Scale bar is 2 cm.

Text-fig. 6. Left mandible of *Khoratpithecus piriyai* (MFT-K181). A: Occlusal view. B: Inferior view. C: Buccal view. D: Lingual view. E: Anterior view. F: Posterior view. (A-F) photographic image. Scale bar is 2 cm.

Text-fig. 7. Morphology of roots of *Khoratpithecus piriyai* (MFT-K181). A: Inferior view. B: Left buccal view. C: Left lingual view. Images are digital renderings of 3D virtual model generated from µCT scan data. Scale bar is 2 cm.

Text-fig. 8. Left maxilla of *Khoratpithecus piriyai* (MFT-K180). A: Occlusal view. B: Superior view. C: Left buccal view. D: Left lingual view. E: Anterior view. F: Posterior view. (A-F) photographic image. Scale bar is 2 cm.

Text-fig. 9. Morphology of roots of *Khoratpithecus piriyai* (MFT-K180). A: Superior view. B: Left buccal view. C: Left lingual view. Images are digital renderings of 3D virtual model generated from µCT scan data. Scale bar is 2 cm.

Text-fig. 10. Bivariate plot on mesiodistal length versus buccolingual breadth (in mm) of new *Khoratpithecu*s compared with other Asian Hominoids. A: lower first molars. B: lower second molars. C: upper first molars. D: upper second molars. MFT-K177, MFT-K180 and MFT-K181 (*Khoratpithecus piriyai*) and MFT-K178 (*Khoratpithecus magnus* n. sp.) data from Table 2; MFT-K176 (*K. piriyai* data from CHAIMANEE et al. (2019); *K. piriyai* data from CHAIMANEE et al. (2004); *K. ayeyarwadyensis* data from JAEGER et al. (2011); *Sivapithecus* spp. data from PREUSS (1982), KELLEY (1988) and BHANDARI et al (2018); *Indopithecus* and *Gigantopithecus* data from SIMONS & CHOPRA (1969), and *Pongo* data from BHANDARI et al (2018).

Text-fig. 11. Mandibular fragment of *Khoratpithecus magnus* n. sp. (MFT-K178). A: Occlusal view. B: Inferior view. C: Anterior view. D: Posterior view. E: Left lateral view. F: Right lateral view. (A-F) photographic image. Scale bar is 2 cm.

Text-fig. 12. Morphology of roots of *Khoratpithecus magnus* n. sp. (MFT-K178). A: Inferior view. B: Left buccal view. C: Left lingual view. Images are digital renderings of 3D virtual model generated from µCT scan data. Scale bar is 2 cm.

Text-fig. 13. Mandibular fragment of *Khoratpithecus* sp. (MFT-K179). A: Occlusal view. B: Inferior view. C: Anterior view. D: Posterior view. E: Left lateral view. F: Right lateral view. (A-F) photographic image. Scale bar is 2 cm.

Text-fig. 14. Morphology of roots of *Khoratpithecus* sp. (MFT-K179). A: Inferior view. B: Right buccal view. C: Right lingual view. Images are digital renderings of 3D virtual model generated from μCT scan data. Scale bar is 2 cm.

Fig. 1

Fig. 2

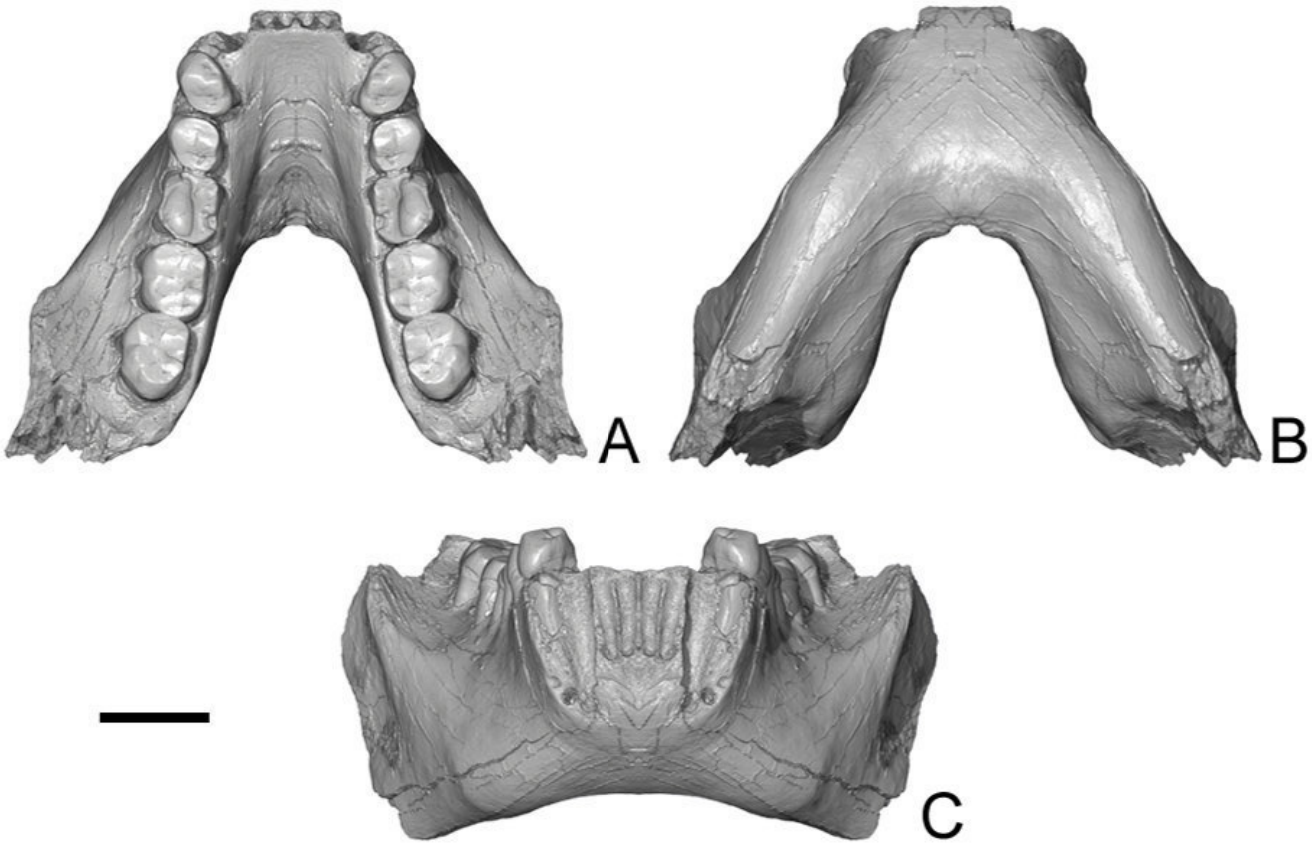

Fig. 3

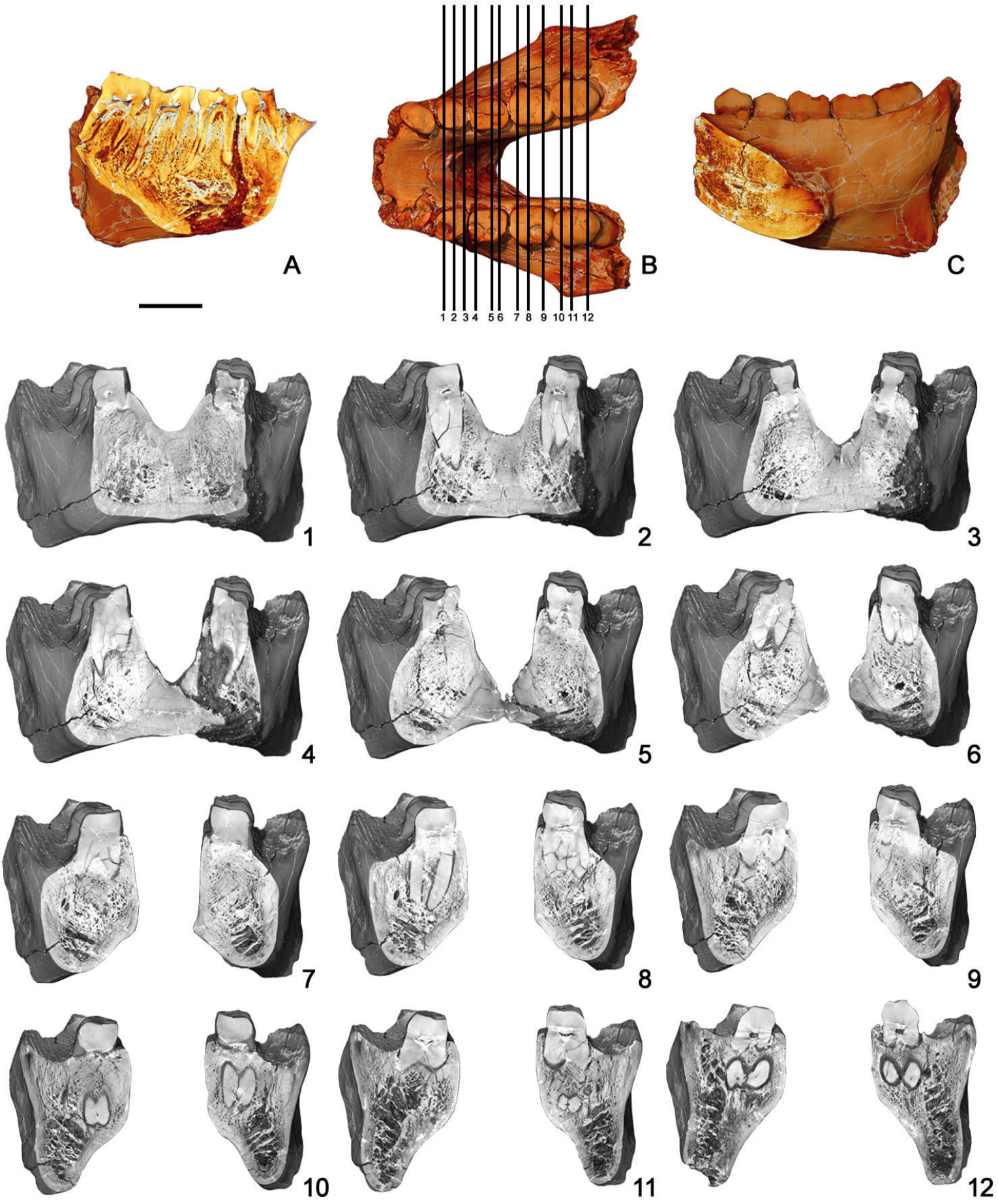

Fig. 4

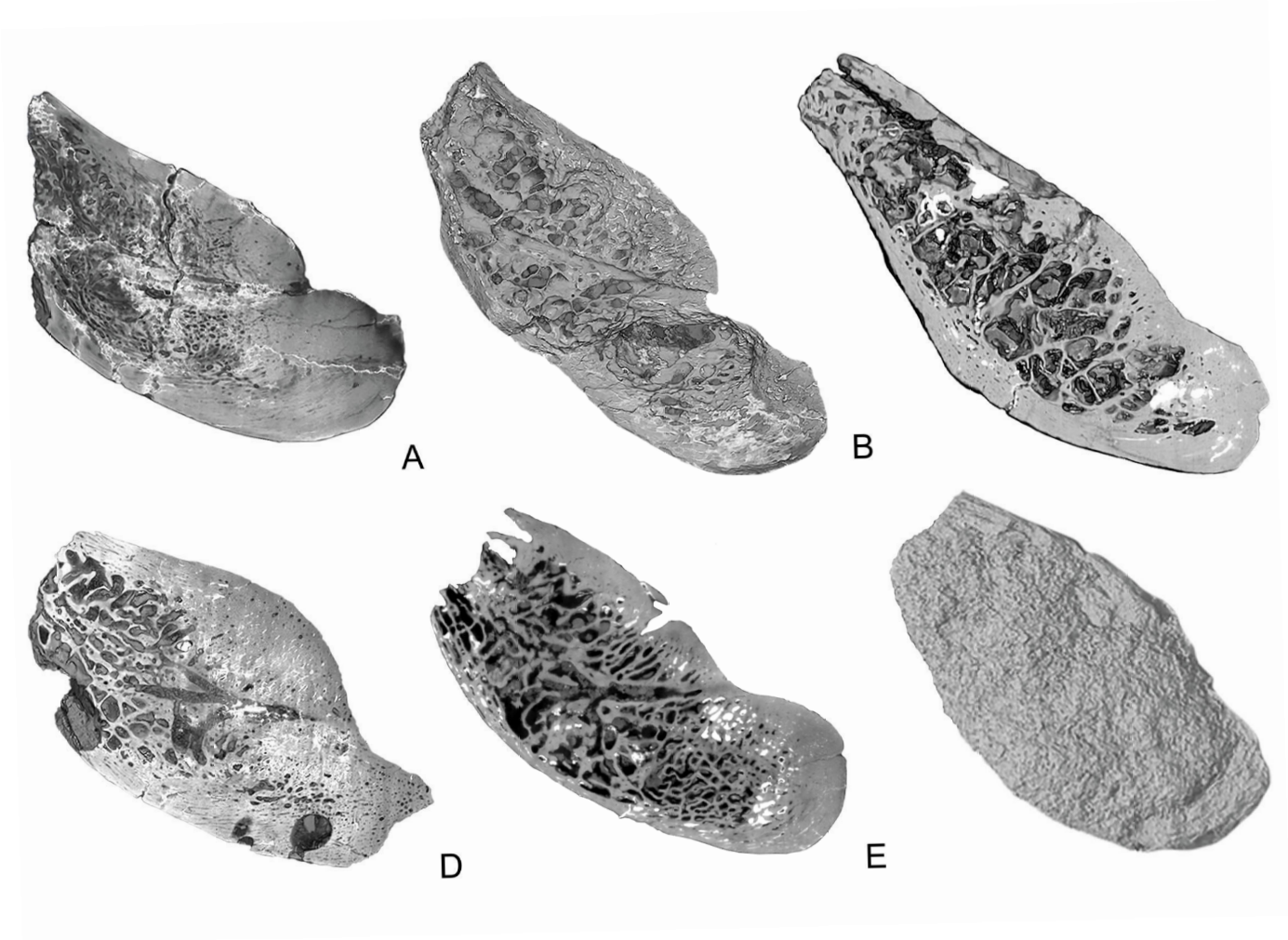

Fig. 5

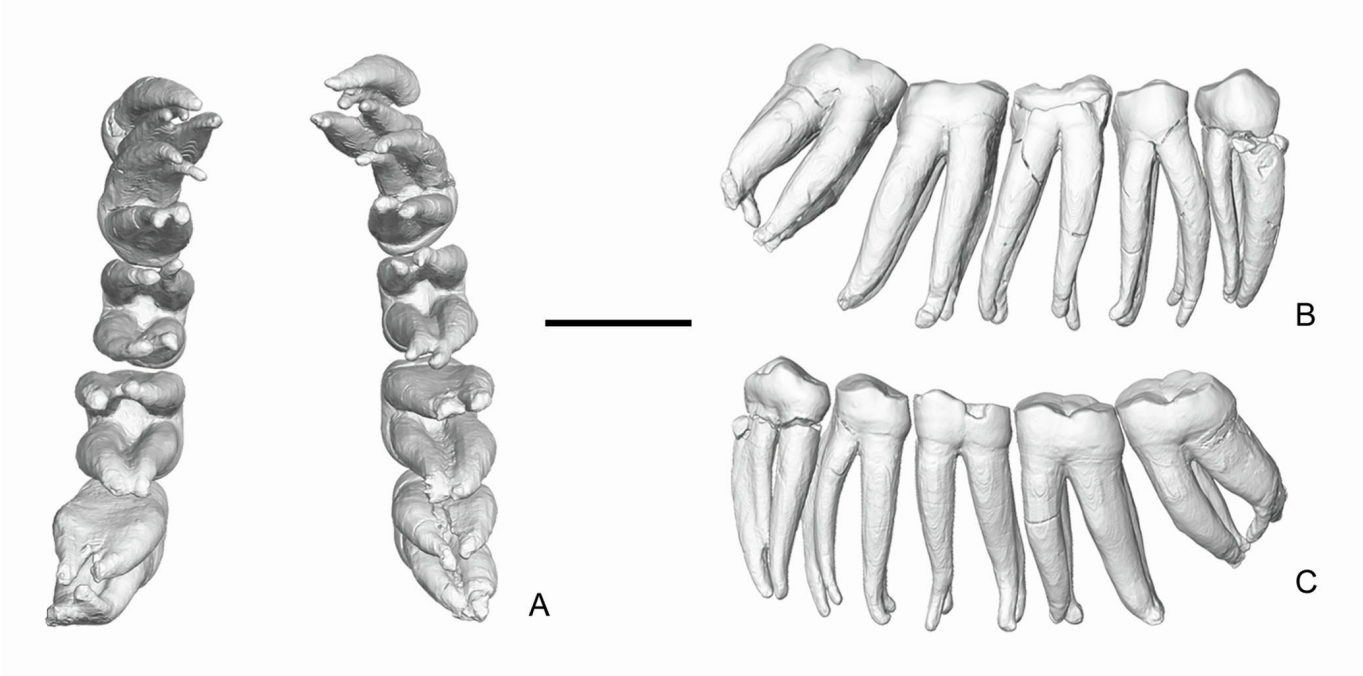

Fig. 6

Fig. 7

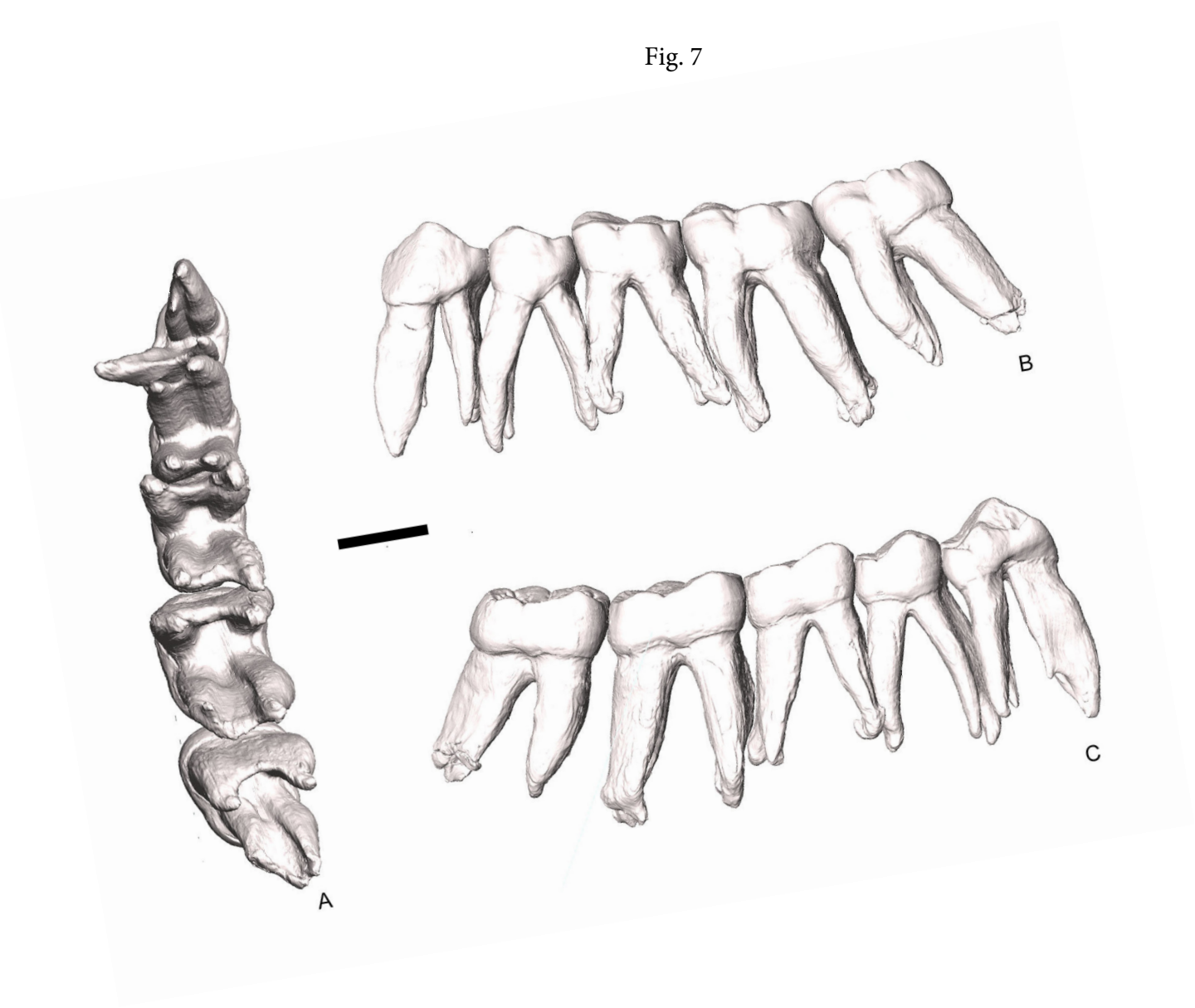

Fig. 8

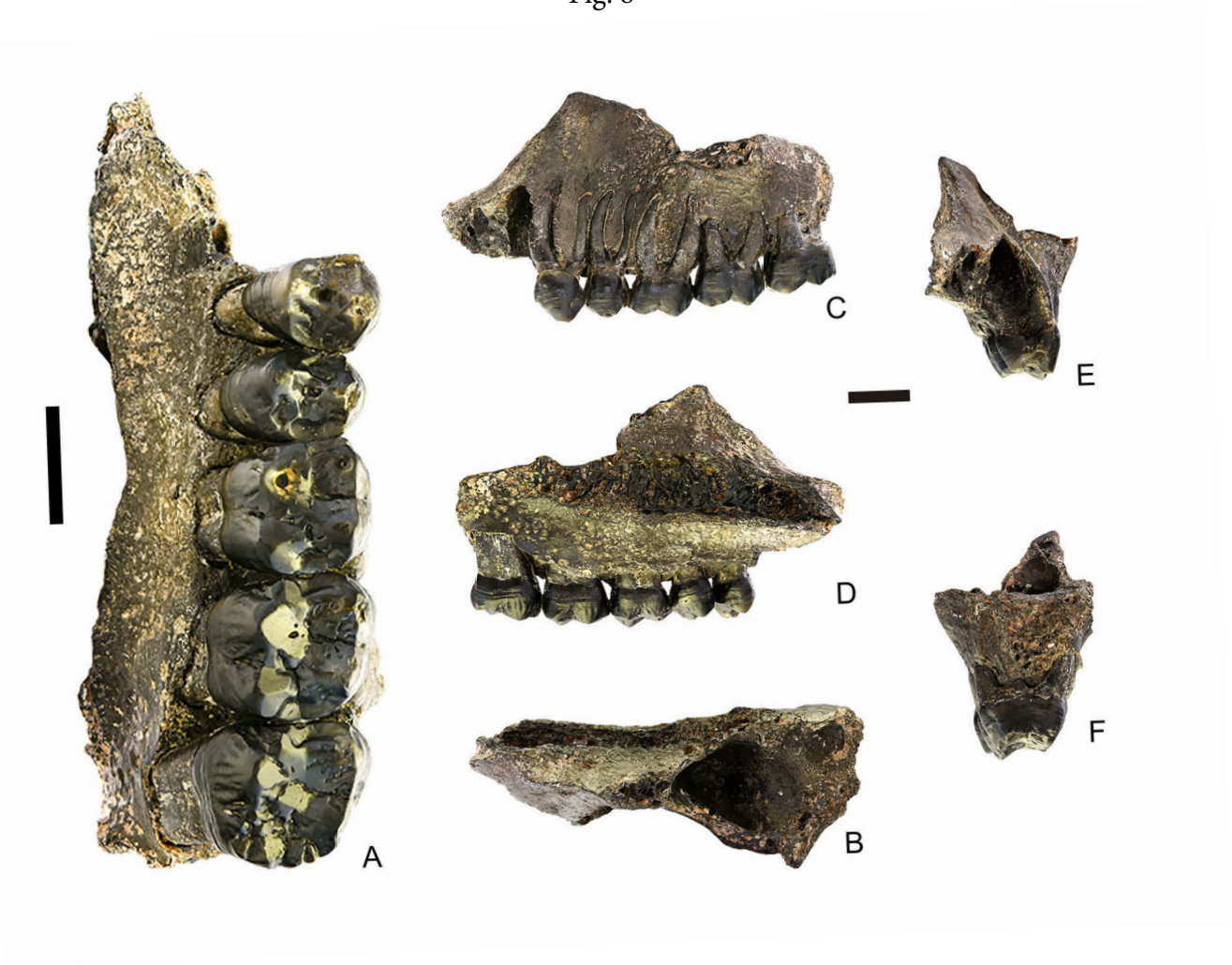

Fig. 9

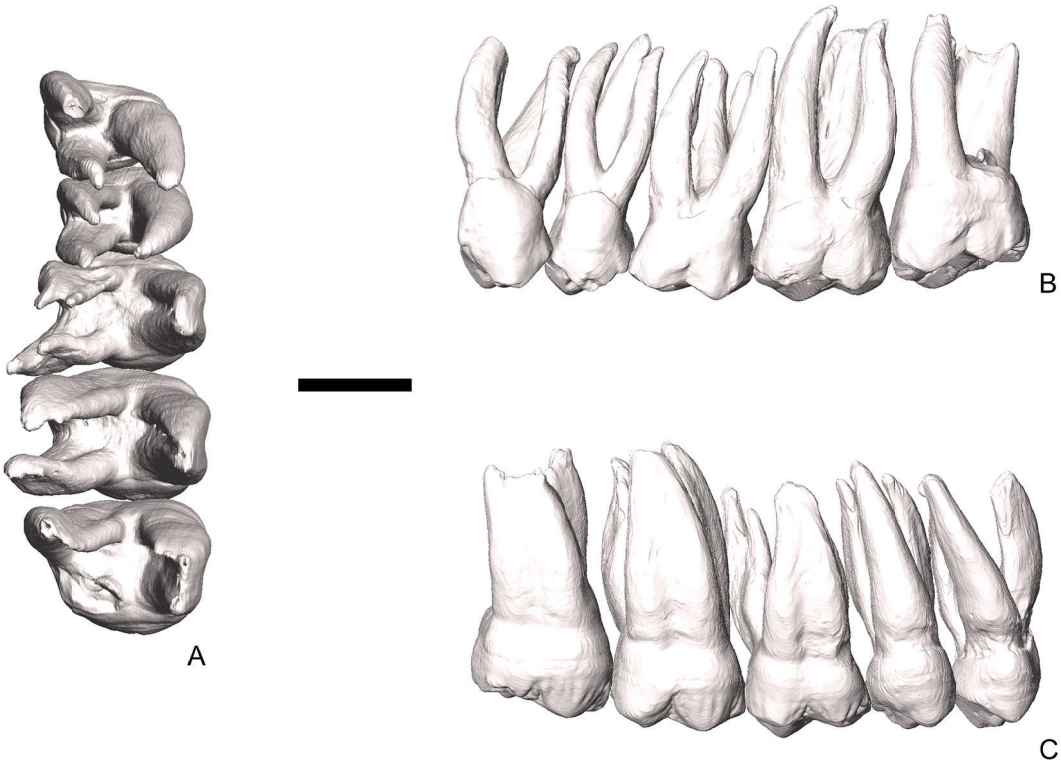

Fig. 10

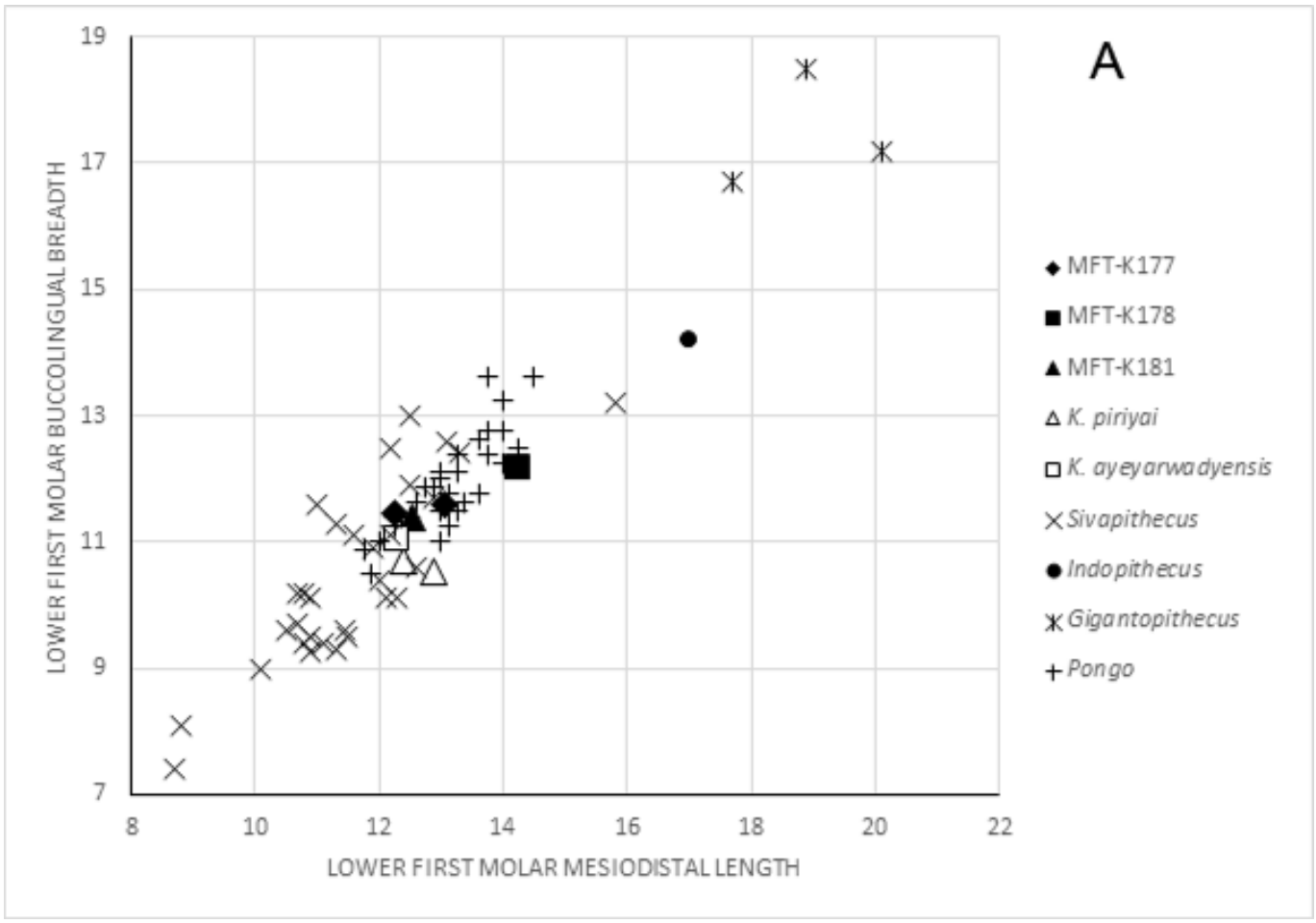
A
LOWER FIRST MOLAR BUCCOLINGUAL BREADTH
LOWER FIRST MOLAR MESIODISTAL LENGTH
19
17
15
13
11
9
7
8
10
12
14
16
18
20
22
MFT-K177
MFT-K178
MFT-K181
K. piriyai
K. ayeyarwadyensis
Sivapithecus
Indopithecus
Gigantopithecus
Pongo

Fig. 10

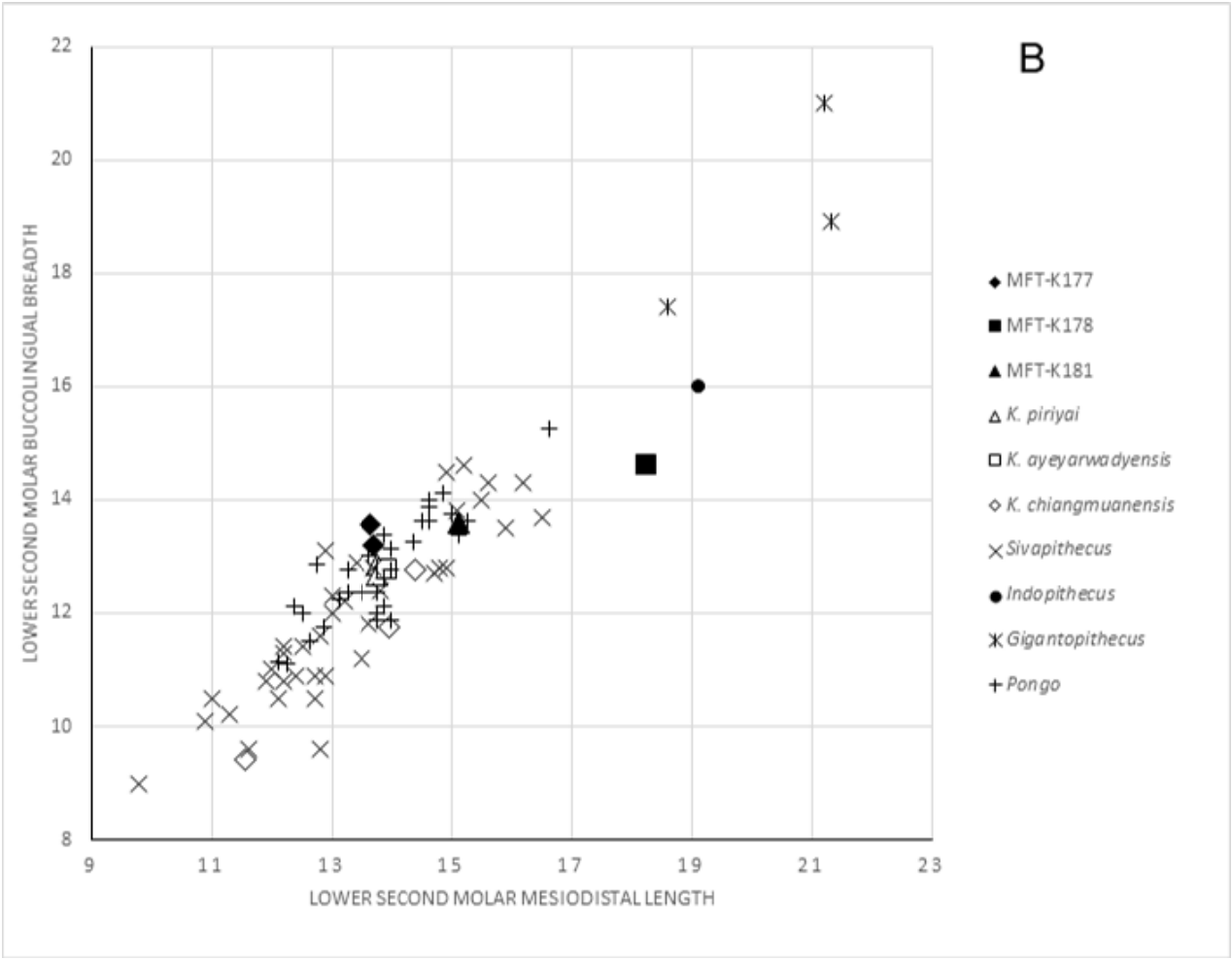
B
LOWER SECOND MOLAR BUCCOLINGUAL BREADTH
LOWER SECOND MOLAR MESIODISTAL LENGTH
22
20
18
16
14
12
10
8
9
11
13
15
17
19
21
23
MFT-K177
MFT-K178
MFT-K181
K. piriyai
K. ayeyarwadyensis
K. chiangmuanensis
Sivapithecus
Indopithecus
Gigantopithecus
Pongo

Fig. 10

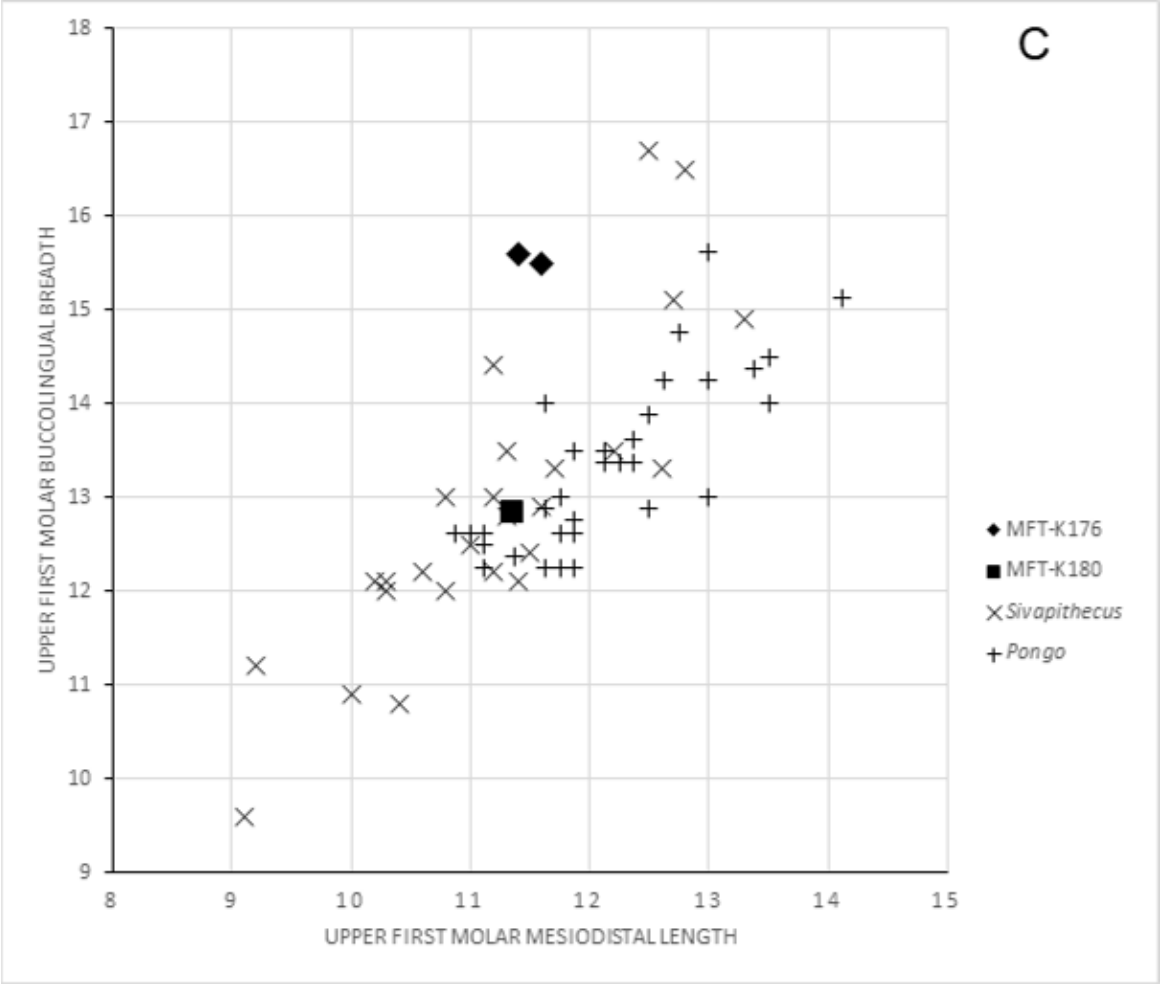
C
UPPER FIRST MOLAR BUCCOLINGUAL BREADTH
UPPER FIRST MOLAR MESIODISTAL LENGTH
18
17
16
15
14
13
12
11
10
9
8
9
10
11
12
13
14
15
MFT-K176
MFT-K180
Sivapithecus
Pongo

Fig. 10

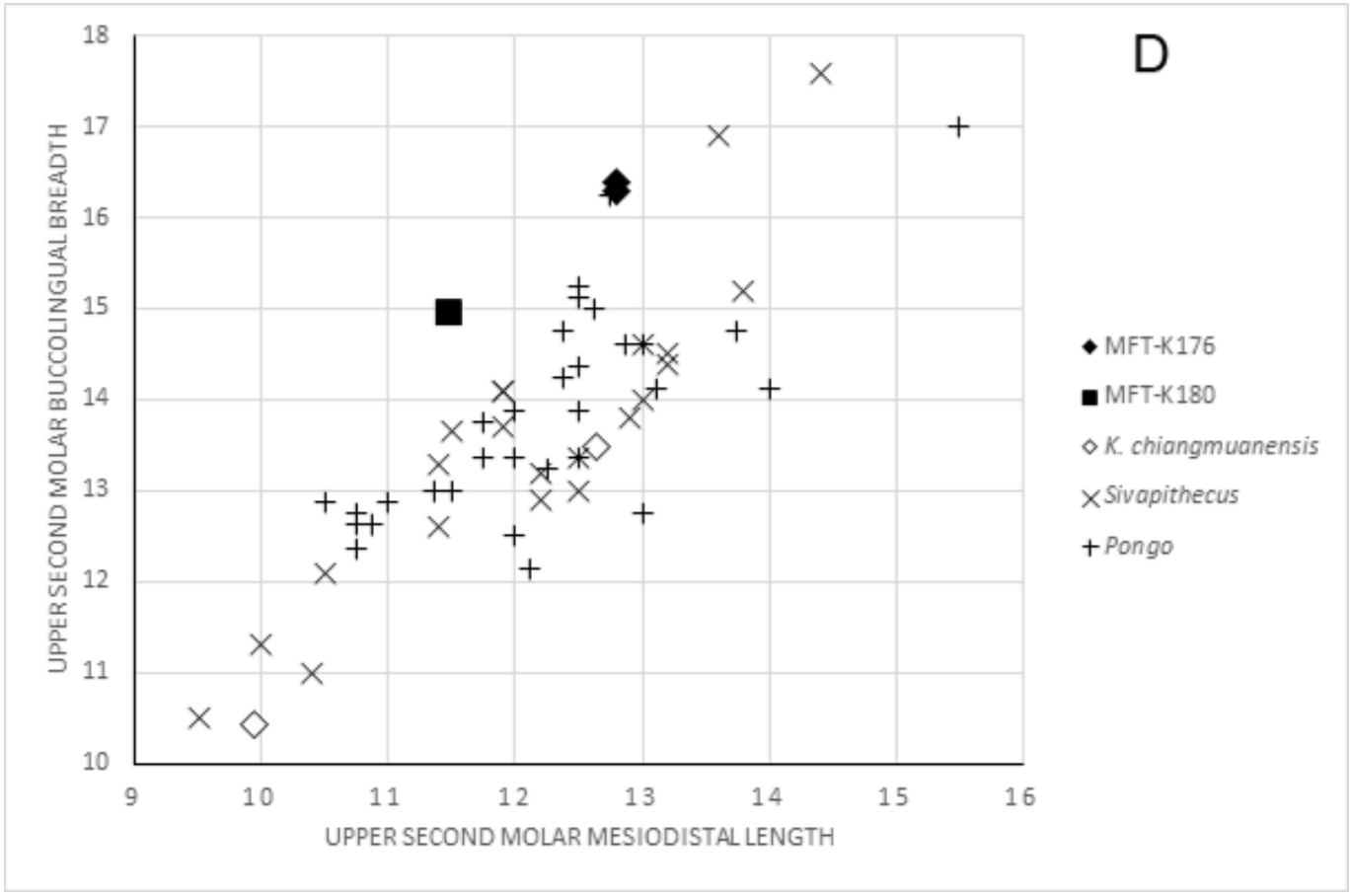
D
UPPER SECOND MOLAR BUCCOLINGUAL BREADTH
UPPER SECOND MOLAR MESIODISTAL LENGTH
18
17
16
15
14
13
12
11
10
9
10
11
12
13
14
15
16
MFT-K176
MFT-K180
K. chiangmuanensis
Sivapithecus
Pongo

Fig. 11

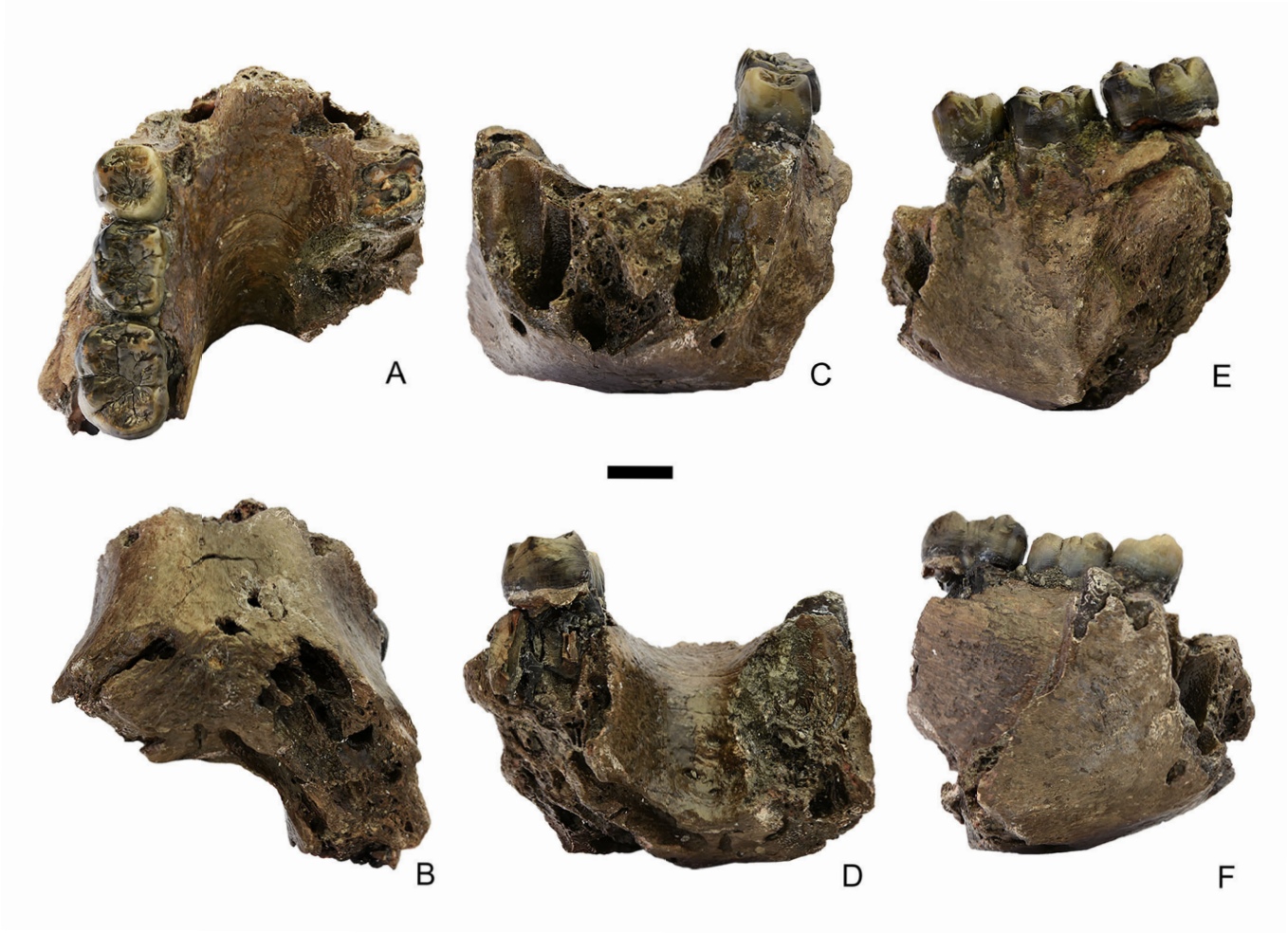

Fig. 12

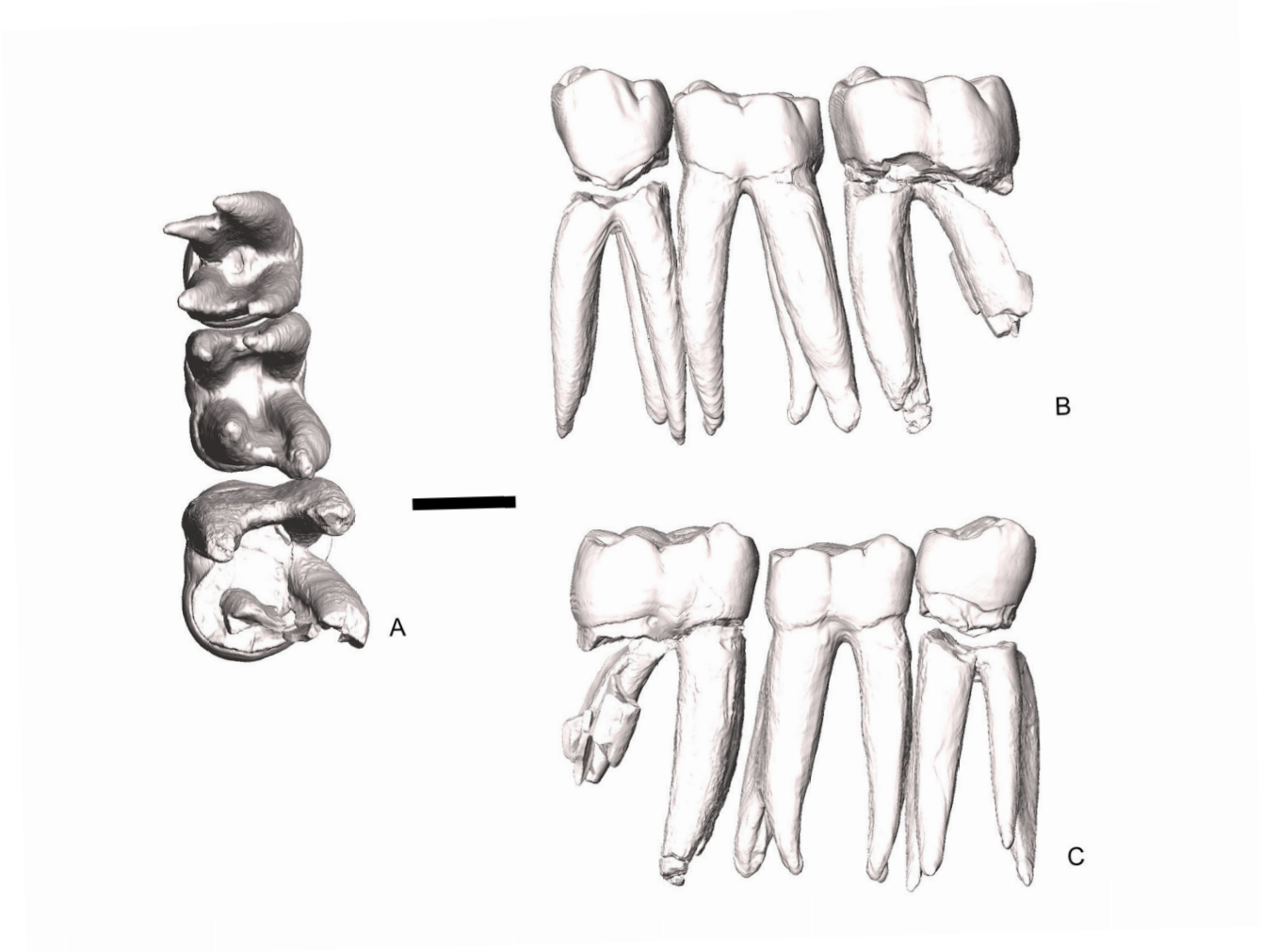

Fig. 13

Fig. 14